ENHANCING THE RETENTION OF THERAPEUTIC CELLS USING NOVEL BIOMATERIALS

MEGAN DUTCHER

THESIS SUMBITTED TO THE UNIVERSITY OF OTTAWA IN PARTIAL
FUFILLMENT OF THE REQUIREMENTS FOR THE DEGREE OF

MASTER OF SCIENCE

Department of Physics
Faculty of Science
University of Ottawa

STATEMENT OF ORIGINALITY

The content presented here is the product of the author at the University of Ottawa under the supervision of Professor Dr. Michel Godin.

In partial fulfillment of the requirements for the degree of Master of Science (Physics) at the University of Ottawa, this work was presented in the Ottawa Carleton Institute of Physics Graduate Symposium on Friday May 14, 2021, as “Enhancing the Retention of Therapeutic Cells Using Novel Biomaterials”.

STATEMENT OF CONTRIBUTIONS

Due to the collaborative nature of the work, some of the work presented in this thesis is not my own. The RGD-modified material that is used here to encapsulate cells was produced by Fan Wan, PhD from the Harden Lab at the University of Ottawa. Simon Chewchuck, PhD acquired the confocal images presented here.

Text presented in this document is an original body of work written by the author. All figures were produced by the author. The microfluidic design used in these experiments was originally designed by Nicolas Cataford, MASc. Preliminary experimental design was designed by Ainara Benavente-Babace, PhD. The LabVIEW programs used for temperature and pressure controls were developed by Michel Godin, PhD. Cell culture, device fabrication, sample preparation, data acquisition, and data analysis were all completed by the author.

ACKNOWLEDGEMENTS

I want to thank my supervisor, Dr. Michel Godin, for providing guidance throughout this project. His help with providing resources, training, and guidance with experimental design and analysis was crucial to my success with this project. I enjoyed working in his lab, in the supportive and collaborative environment he has created. I am very thankful for the opportunity to work in his lab which has been a very positive experience, where I have gained incredibly valuable experience and skills.

I also want to thank Dr. Ainara Benavente-Babace for her work previously on this project. She provided invaluable notes and preliminary research for this modified agarose project, fielded lots of questions from me as I got started and I am incredibly grateful for all of it.

I also could not have completed this work without the constant support of my current lab members Nick Soucy, Kaitie Kean, and Dr. Simon Chewchuck. Nick provided training for all equipment used in this project and was always someone I could bounce ideas off of throughout my project, providing extremely valuable expertise. It was a pleasure to work with everyone that came through the lab during my time working there.

Dr. James Harden and Dr. Fan Wan also provided critical support with the production of RGD-modified agarose, and I am very thankful for their help and guidance on all matters regarding this material.

Lastly, I want to thank my family, John, Heather, and Lauren Dutcher for supporting me throughout the last two years.

CONTENTS

Table of Contents

LIST OF FIGURES

LIST OF EQUATIONS

(1) $$\mathrm{Ca} = \frac{\eta v}{\sigma}$$

(2) $$We = \frac{\rho U^2 D_h}{\sigma}$$

(3) $$p(k, \lambda) = \frac{\lambda^k e^{-\lambda}}{k!}$$

(4) $$\lambda = \frac{\phi_s \bar{v}_d}{\bar{v}_c} = c_c V$$

(5) $$\%\ \text{cumulative egress} = \frac{\text{occupancy}_{2\text{h}} - \text{occupancy}_{24/48\text{h}}}{\text{occupancy}_{2\text{h}}}$$

(6) $$\text{occupancy} = \frac{\#\ \text{total encapsulated cells}}{\#\ \text{total microcapsules}}$$

(7) $$\%\ \text{viability} = \frac{\#\ \text{live cells}}{\#\ \text{total cells}}$$

(8) $$\%\ \text{cells attached} = \frac{\#\ \text{attached cells}/\text{microcapsule}}{\#\ \text{egressed cells}/\text{microcapsule}}$$

(9) $$\#\ \text{attached cells}/\text{microcapsule} = \frac{\#\ \text{attached cells}_{24/48\text{h}}}{\#\ \text{total microcapsules}_{24/48\text{h}}}$$

(10) $$\#\ \text{egressed cells}/\text{microcapsule} = \frac{\#\ \text{live encap. cells}_{2\text{h}} \times\ \%\ \text{cumulative egress}_{24/48\text{h}}}{\#\ \text{total microcapsules}_{2\text{h}}}$$

ABSTRACT

Cell-based therapeutic strategies are becoming increasingly popular in treating many diseases that historically have been challenging to treat. Strategies involving injections of healthy cells into damaged tissues have benefits over current transplantation and drug strategies because they eliminate the need for long term use of immunosuppressing drugs and reduce the issues of limited availabilities of tissue donors. However, there are still major issues with current cell-based strategies, including limited cell engraftment and retention at the site of injury. Recent studies show that a very limited number of cells are retained at the site of injection, but therapeutic effects as still observed. Examples include improved cardiac function when cells are used to treat myocardial infarctions[1–3], improvements are observed for treating retinal degenerative diseases[4], and increased bone formation in bone regeneration strategies[5], as well as improvements for many other disease treatments. Encapsulating cells in hydrogel microcapsules has been shown to increase cell retention significantly, as well as protect the cells from any unwanted, negative immune responses from the host. However, previous studies showed that long-term retention of encapsulated cells is still reduced due to cell escape or egress from the hydrogel microcapsules.[6] Once escaped, these cells are free floating, and surrounding vasculature and blood flow clear the cells from the site quickly.[3,7,8] The proposed strategy of reducing cellular clearance is through modifying the encapsulation material with cell binding domains, specifically by adding a peptide sequence of arginine, glycine, and aspartate (RGD). These binding sites allow the cells to adhere to the outside of the microcapsules after they have escaped. Attachment to the microcapsules means the egressed cells are not free floating and

therefore will not be cleared away from the site of injury as easily, therefore leading to long-term retention at the site of injury. Long-term retention is believed to increase efficacy of these cell-based treatments.

Cellular attachment to hydrogel microcapsules was investigated by encapsulating cells in regular agarose and in RGD-modified agarose. Encapsulation was conducted using a microfluidic device to create uniform, monodisperse agarose microcapsules containing cells. These encapsulated cells were then studied using timepoint fluorescence microscopy to determine cell viability, microcapsule occupancy, cell escape from microcapsules and cellular adhesion onto the microcapsules. These quantities were assessed at three timepoints after encapsulation - 2 h, 24 h, and 48 h - to investigate whether cell behaviour was changing with time. Different environmental conditions were investigated as well, to imitate different cellular environments that may affect cell adhesion to a material. Samples were studied in cell culture treated dishes as well as poly(2-hydroxyethyl methacrylate) (pHEMA) coated dishes to simulate environments in which cells can adhere to surrounding surfaces, and environments in which adhesion is inhibited.

The results presented here show that RGD-modified encapsulation material does increase cell attachment to the outside of microcapsules. I show that this cellular behaviour occurs with multiple cell types, including therapeutically relevant cells such as explant derived cardiac stem cells, and human umbilical vein endothelial cells. Cells behave quite differently in regular, unmodified agarose, where almost no cell attachment is observed. I show that this novel biomaterial does not negatively impact viability of encapsulated cells, and can be used inside semi-automated, scalable microfluidic devices for cell encapsulation. The research presented here shows promise for eliminating some of the limitations currently observed in many cell-based

therapeutic strategies and it is hypothesized that the use of this novel biomaterial for cell encapsulation will lead to increased therapeutic effects *in vivo* due to increasing cellular retention at the site of injury.

1 INTRODUCTION

1.1 Cell-based Therapeutic Strategies

Cell-based treatments for repairing injured tissues have been of great interest over the past few decades. Tissues are damaged in many ways, including physical trauma, cancer, and ailments like heart disease, lung disease, and many, many more. When tissues are significantly damaged, there is a major loss of cells, which means a major loss of tissue functions and a significant negative impact on the proper function of the systems in which these tissues occur. There are a few general therapeutic treatments options for regaining the function lost from tissue damage, including drugs, transplants, and delivery of healthy cells. This latter option, cell-based treatments are the focus of this research.

The general strategy in cell-based therapies involves the same basic process: healthy cells are injected into damaged tissues. These healthy cells can come either from the patient with the damaged tissue, referred to as an autologous treatment, and this treatment is possible when healthy tissues are available and can be harvested from the patient.[9] Cells can also be derived from a different donor, known as an allogeneic treatment, and are commonly used when the patient's own tissues cannot be harvested.[9] Allogeneic treatments can lead to possible negative immune responses since these cells do not originate in the patient. Due to limited sources for healthy cells, they are typically harvested, then expanded *in vitro* to ensure a sample large enough to provide the necessary therapeutic effect.[10] With enough cells for treatment, they are

then injected into the site of damage to provide therapeutic effects and repair the damaged tissue.

Therapeutic effects are achieved through two different modes of action: through engraftment and integration of injected cells into damaged tissues, or through paracrine signalling enhanced by injected therapeutic cells.[11] Engraftment, which occurs when the injected cells adhere to the site of damage and replace the damaged cells, is a slow process but can give long term benefits. The other mechanism, paracrine signalling, involves stimulating endogenous self-healing processes from products secreted by the injected cells such as growth factors, cytokines, and other soluble factors. The injected cells help trigger and speed up these innate processes, leading to faster, more robust effects.[12]

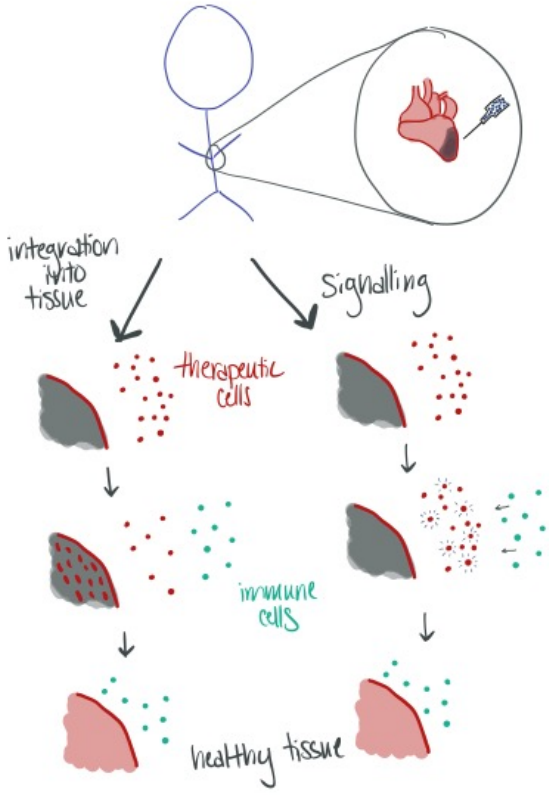

Figure 1 Schematic of cell-based therapies. Cells injected into damaged heart tissue, with two pathways of repair: integration involving cell engraftment into surrounding tissue to replace damaged cells, or paracrine signalling involving cell-to-cell communication to initiate endogenous self-healing processes.

These cell-based therapeutic strategies have two major benefits over previous strategies like tissue transplants and drug-based strategies. Transplants require the long-term use of immunosuppressive drugs which leads to lifelong side effects including the reduced ability to fight off common bacterial or viral infections.[11] Another downside to transplantations is the limited availability of donor organs and donor tissues.[11] Drug treatments are expensive, and their use is needed long-term. Cell-based strategies circumvent these issues and show great promise for treating tissue damage that has long been considered irreparable.

1.2 Cell Encapsulation Techniques

Although cell based-therapeutic strategies have been in use for decades, there are still many issues involved with their efficacy and use. There are two main issues that lead to reduced efficacy of these treatment options: low engraftment and low retention of cells around the area of damage. One reason that these strategies have low engraftment is due to negative immune responses toward the injected cells. The patient's immune system will often label these new, healthy cells as foreign and try to remove them from the body. Low retention is caused by the constant flow of surrounding fluids and vasculature that quickly and easily clear the free-floating

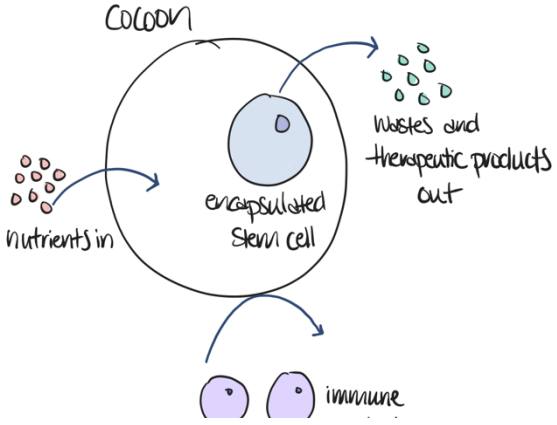

Figure 2 Cell encapsulation in hydrogel microcapsule. Surrounding hydrogel keeps negative immune responses away from injected cell, but porous structure of gel allows diffusion of nutrients and signals in while wastes and therapeutic products can diffuse out.

cells from the site.[13,3] This clearance does not allow enough time for cells to engraft and reduces retention at the same time. Both issues result in cell removal from the damaged site and therefore they are no longer able to provide the therapeutic effect that is needed.

One method that helps improve both the engraftment and retention is cell encapsulation inside a hydrogel. Encapsulation inside of a hydrogel matrix provides the cells with a protective coating, keeping large immune cells away, while allowing necessary small molecules to diffuse into and out of the cells' immediate environment.[14] Encapsulation allows for cell-based treatments without the use of immunosuppressive drugs, which have many unwanted side effects, and can negatively affect the outcome of these therapies.[14] Cells need nutrients to survive, and they produce wastes that need to be removed from their environment; the porous structure of most hydrogels allows for the diffusion of these small molecules. Since the cells are encapsulated in larger volumes of hydrogel, cell retention is increased because the vasculature and blood flow cannot move these larger objects unlike the smaller cells, as shown in recent studies.[3] Hydrogels can also be designed to stick better at the site of injection, so that they have limited mobility *in vivo*.

Two main methods of cell encapsulation exist: macroencapsulation where many cells are encapsulated together in a larger volume of hydrogel, and microencapsulation, where individual cells are encapsulated in much smaller volumes of hydrogel. The latter, microencapsulation, allows for more control over the specific properties of the encapsulated cells, increases surface area for better solute diffusion, and the smaller microcapsules typically have higher mechanical strength and are therefore more durable.[14] Microcapsules are also easier to inject using a syringe/ needle into the site of interest, compared to larger pieces of hydrogel.

Techniques to microencapsulate cells have been used for over 50 years, with the first cells microencapsulated in 1966, where erythrocytes were encapsulated in nylon spheres.[14] As technologies have progressed, many new methods of encapsulating cells have emerged that allow more control over hydrogel properties, allow a variety of different gelling mechanisms for different types of hydrogels, and use gentle conditions necessary for the cells within the hydrogel.

Microencapsulation strategies include vortex-based approaches, electrospray techniques and microfluidic-based methods. Vortexed-based approaches involve mixing two immiscible solutions together in a container that is vortexed to create an emulsion (similar to mixing salad dressing), then the solution undergoes gelation according to the specific hydrogel mechanism (thermal, chemical gelation, etc.).[15] Centrifugation is then used to remove the gelled microcapsules from the other phase. Electrospraying techniques involve spraying hydrogel solution through a small nozzle and down into a solution where the hydrogel is gelled.[16] The fluid solution is maintained at a high electrical potential and electrostatic repulsion disrupts the surface tension of the fluid at the nozzle, where the fluid drops down into a grounded solution.[16]

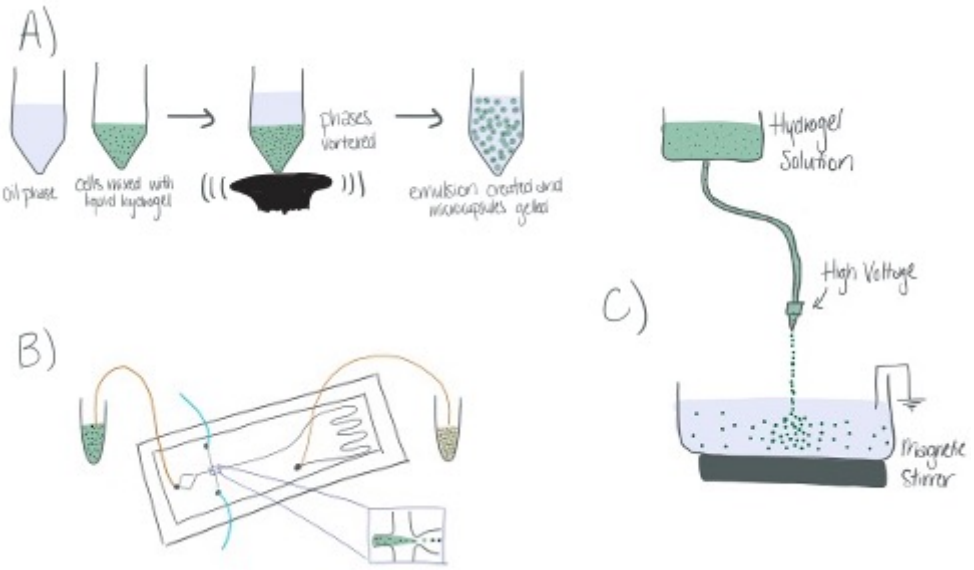

Figure 3 Methods of microencapsulation of cells. A) vortex-based method B) microfluidic based method C) electrospraying encapsulation method.

Both the vortex-based and electrospraying methods do not allow good control over the size of the microdroplets formed and can induce high shear rates to the hydrogel. Since microfluidic encapsulation allows for precise control over microdroplet size, gentle formation of the droplets around the enclosed cells, and thermal gelation to occur, it was chosen for this project.

1.3 Microfluidics for Cell Encapsulation

Microfluidic devices allow you to manipulate very small (on the order of nL) volumes of fluids through small channels. Due to the small volumes and slow velocities within these systems, the fluid flow remains strictly laminar, meaning that you have very precise control over flow characteristics and droplet formation. Droplet-base systems are typically favourable over continuous flow systems due to the ease of manipulating individual droplets and scalability. Droplet-based microfluidic systems allow for a semi-automated, scalable process of creating highly monodisperse hydrogel microdroplets.[17] Microfluidic setups can be easily made to incorporate simple methods for gelling different types of hydrogels that use a variety of different gelling methods. Most microfluidic devices are made of poly(dimethyl)siloxane (PDMS) due to its cost effectiveness, and its mouldability, though other materials have been used such as glass [18] and silicon [19].

The basic model of a droplet-based microfluidic device operates by driving two immiscible fluids into the device where their flow paths meet, where surface tension and shear forces are used to break apart one fluid stream creating an emulsion. Systems like the one used in this project use a pressure-driven system to force the fluids through the devices. Most microfluidic device technology uses a water-in-oil emulsion system, but other systems, such as oil-in-water,

or more complicated systems like water-in-oil-in-water, can be created as well. The resulting droplets are then typically gelled on chip, using a mechanism (e.g., thermal gelling, chemical crosslinking, etc.) that is specific to the choice of hydrogel.

There are different main methods of droplet formation used in microfluidic devices, namely cross-flow methods, flow focussing methods, and co-flowing methods.[20] The cross-flowing droplet method has two channels oriented perpendicular to each other and intersecting at a T-junction. Figure 4 A shows this intersection with the continuous phase moving through the upper horizontal channel and the dispersed phase moving upward toward the continuous channel. As the fluid moves through the device, the fluid coming from the bottom will be broken up due to shear stresses, interfacial tension, and pressure gradients[20], which creates an emulsion downstream. A device that uses the flow focussing design (Figure 4 B), involves 3 channels intersecting each other at 90˚ angles. The top and bottom channels contain the continuous phase, most commonly oil, while the horizontal, middle channel contains the dispersed phase, usually an aqueous phase for an oil-in-water emulsion. As the fluids move toward the intersection, a small nozzle forces the two phases together and the continuous phase pinches the dispersed phase to form droplets. The third main type of microfluidic geometry is the co-flow design. This device uses two capillaries – one smaller capillary inside another larger capillary, shown in Figure 4 C. The phase moving through the inner capillary is broken up by interfacial

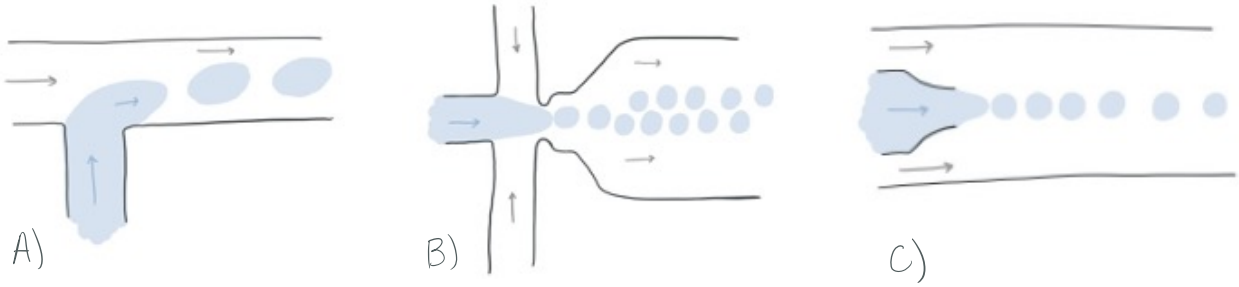

Figure 4 Three geometries for droplet formation used within microfluidic devices. A) cross flow geometry, also known as T junction geometry, B) flow focussing nozzle, and C) co-flow geometry.

tension and shear stressed from the flow of the continuous phase flowing in the same direction around the inner phase.[21]

The flow focussing device design was chosen for my project because of its high-throughput, and high monodisersity. Droplet monodispersity is slightly improved for the flow focussing design since the shear forces on the aqueous phase are symmetric on either side of the dispersed phase, whereas the shear forces for the cross-flow geometry are one-sided.[22]

There are three main regimes for droplet formation that are mainly determined by the Capillary number and Weber number– dripping, jetting, and continuous flow regimes (shown in Figure 5). The Capillary number is defined as

$$\mathrm{Ca} = \frac{\eta v}{\sigma} \tag{1}$$

where η is the viscosity of the continuous phase (Pa*s), v is the velocity of the continuous phase (m/s), and σ is the surface tension of the water-oil interface (0.001 N/m^2).[20,22,23] The Capillary number is a unitless value and defines the relationship between viscous forces and interfacial tension forces.[24] The Weber number is defined as:

$$We = \frac{\rho U^2 D_h}{\sigma} \tag{2}$$

where ρ is the aqueous fluid density (kg/m^3), U is the mean velocity of aqueous phase (m/s), D_h is the channel hydraulic diameter (m), and σ is the interfacial tension between the two immiscible fluids (N/m). This value measures the relationship between the inertial and interfacial tension forces of the aqueous phase. At lower Capillary numbers (Ca << 1) and low Weber numbers (We << 1), shear forces dominate, and dripping occurs, forming very uniformly sized droplets.[24] As the Capillary number increases (Ca ~ 1 or larger) or the Weber number increases (We ~ 1 or greater),

the viscosity starts to dominate, and jetting and finally a continuous flow occurs.[24] Droplets form in the jetting regime due to Rayleigh-Plateau instabilities along the thread of fluid that is formed (Figure 5 B), but there is less consistency in the size of droplets formed.[23] No droplets are formed during the continuous flow regime, therefore this regime must be avoided. The velocity of the continuous phase is the easiest variable to modify to change the Capillary number, and therefore the regime of droplet formation. Altering the continuous phase inlet pressure directly affects the continuous phase velocity.

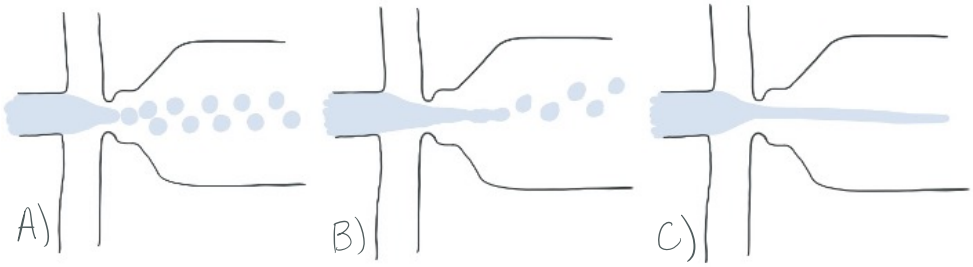

Figure 5 Three regimes inside a microfluidic device at the nozzle during droplet formation. A) dripping regime where uniform, monodisperse droplets are formed. B) Jetting regime where droplets form but due to Rayleigh-Plateau instabilities, these droplets are less uniformly sized. C) Continuous flow where no droplets are forming.

1.4 Poisson Distribution

When cells are well mixed into the dispersed phase within the microfluidic device, the cells arrive at the nozzle randomly, with an arrival rate that can be estimated using the concentration of cells in the solution. Because of this random arrival, and the fact that cells arrive at the nozzle independently of each other, the number of cells inside each microdroplet follows a Poisson distribution where single cell encapsulation is preferred. The Poisson distribution is given by:

$$p(k,\lambda) = \frac{\lambda^k e^{-\lambda}}{k!} \quad (3)$$

where λ is the average number of cells per droplet volume , and k is the number of particles in a droplet.[17,23,25] The average number of cells per droplet volume (in other words, the average occupancy of a droplet λ), can be represented in terms of the concentration of cells in the solution, a quantity that is easily modified during experimentation:

$$\lambda = \frac{\phi_s \bar{v}_d}{\bar{v}_c} = c_c V \quad (4)$$

where ϕ_s is the volume fraction of cells in the pre-encapsulated solution, $\bar{v}_d$ is the average droplet volume (L), $\bar{v}_c$ is the average cell volume (L), c_c is the cell concentration in pre-encapsulated solution (particles/L), and V is the volume of a microdroplet (L).[23]

1.5 Encapsulation Materials

Many different hydrogels have been used as the encapsulation materials for cell encapsulation purposes. Early studies of cell encapsulation used materials such as collagen, fibrin, and alginate.[26–28] These materials have the benefit of being natural and biodegradable, but ultimately had issues with mechanical properties, and degradation rates that were hard to control.[29] It became clear that any material used for cell encapsulation needed to exhibit properties that were very similar to the tissues from which the encapsulated cells originated.

Some of the main properties that are important for cell viability within a material include biocompatibility, gelation mechanism, and porosity. These general properties have large effects on the encapsulated cells, but other properties are important too, such as mechanical strength of the material, degradation rate and cell adhesiveness. Any material that forms the immediate

environment around a cell must first and foremost be biocompatible, meaning that the material itself does not cause any cytotoxic effects to the cells. Natural materials such as collagen, fibrin, chitosan, and alginate are chosen for this reason. The gelation mechanism for any encapsulation material must also be gentle enough on the cells so that it does not cause extended stress and lead to reduced cell viability. The hydrogel must also have reasonable mechanical strength after gelation so that it can withstand the mechanical stresses imposed during product manipulation and injection. Another extremely important characteristic of any encapsulation material is that it is porous enough that nutrients, metabolites, and wastes can easily diffuse into and out of the hydrogel to ensure the survival of the cells within the material. As previously stated, paracrine signalling is extremely important in producing therapeutic effects of cell-based therapies. The diffusion of these cell signals through the encapsulation material is therefore critical for these treatments. The encapsulation matrix surrounding the cell also protects the cells from negative effects of the host's immune system. Often these strategies are allogeneic cell therapies meaning the cells originate from a donor that is not the recipient of the therapy. This means that the host's immune system can quickly try to eliminate these cells as foreign objects. Many of the hydrogels mentioned here are ideal for this purpose as they have pore sizes small enough to keep large immune cells (roughly 10-100 μm diameter[30]) out but large enough for small molecules and signals (molar mass < 100 kDa) to easily diffuse through them. It is very important for the efficacy of these treatments that the injected cells are protected from this negative immune response.

Natural polymers such as alginate[26,31], agarose[3,32,33], collagen[34–36], gelatin[37], hyaluronic acid[38,39], and chitosan[40] have been widely used, as well as synthetic polymers such as poly-ethylene glycol (PEG)[41], and poly(lactic-glycolic acid) (PGLA)[42]. Natural polymers have the benefit

of low toxicity to the cells they are encapsulating as well as to the tissues into which they are injected. These gels have wide ranging gelation mechanisms, from chemical cross-linking[40], to UV sensitive materials[38], to temperature dependent gelation[32]. Typically, cells are mixed with encapsulation material before gelling to ensure proper encapsulation. Therefore, gelling mechanisms cannot be too harsh on the cells. For example, the gelling temperatures for both gelatin and agarose typically lie between the normal working conditions of mammalian cells of 0 – 37 ˚C, which makes them ideal for use with cells. The choice of hydrogel used for cell-based therapies needs to consider all these factors and these different properties will have varying degrees of importance for different applications and for different treatments. A cell treatment for bone regeneration will need very different mechanical and biochemical properties compared to a treatment used for myocardial infarctions. Research into understanding the native environments for common diseases and the mechanical, biochemical, and physical properties of different encapsulation hydrogels is critical for determining the best material for each individual use.

One of the most common hydrogels used for cell encapsulation is alginate. Alginate is a polysaccharide that is found naturally in the cell walls of some species of algae. This polymer is made up of β-D-mannonic acid monomers that are linked through 1,4-glycoside bonds to α-L-glucuronic acid monomers.[43] Alginate forms gels through a chemical cross-linking process when in the presence of divalent cations (usually Ca^{2+}). Its success in cell encapsulation is due to its low cost and ease of cross-linking. One drawback to alginate is that it forms a relatively weak gel, which means that the encapsulated cells can easily and quickly escape the gel, and the alginate gel will dissolve when exposed in the long term to the host's immune system *in vivo*.[14] In some

cases, the gel strength is increased by the addition of a polycation layer surrounding the alginate microcapsule, but this itself can cause an inflammatory response from the host's immune system, which is detrimental to this therapeutic strategy.[14] Another disadvantage to using alginate for cell encapsulation is that it does not possess any cell binding capabilities. Without binding domains, the encapsulated cells will not interact much with the material which can negatively impact viability, proliferation, and differentiation.

Another common cell encapsulation material is collagen. Collagen, which is a major component of the extracellular matrix, is a natural polymer that is very biocompatible, and an ideal candidate for a cell encapsulation material.[44] Collagen molecules are made of three interpenetrating helices consisting of polypeptide strands that are each held together through hydrogen and covalent bonds.[45] Many studies have used collagen for cell encapsulation. From bone substitutes[46], skin replacements[34], and bioengineered tissues[35], collagen has a multitude of uses in cell-based therapies. A major benefit of using collagen for tissue regeneration is that it degrades easily *in vivo*, as shown by a study by Jaques *et al.*[35] where the presence of collagen mixed with inert agarose led to biodegradability of the material, which is often necessary for proper cell engraftment. Without proper control of precise degradation timing, this property can also become an issue, as early degradation or late degradation can lead to issues with engraftment, or proper cell differentiation and growth.[41] Some disadvantages of using collagen for cell encapsulation include its high price, weak mechanical strength, heterogeneity when originating from a natural source, and its difficulty in controlling degradation.[47]

1.6 Agarose

Agarose is another common, relatively inexpensive hydrogel that was ultimately chosen for this project. It is a polysaccharide naturally derived from seaweed, specifically a disaccharide of D-galactose and 3,6-anhydro-L-galatopyranose linked by glycosidic bonds.[32] Agarose is the main component in agar, along with agaropectin. Many of agarose's characteristics are ideal for use with this project, namely its structural and gelling properties. The matrix formed by gelled agarose is very similar to that of the extracellular matrix, a cells natural environment. Creating an environment that closely resembles a natural cellular environment is critical for high cell viability within the encapsulation material. Agarose is thermally responsive, meaning that liquid agarose can quickly be transitioned into its gel state by lowering its temperature.[32] To ensure proper cell encapsulation, gelling is typically completed after mixing with cells, therefore moderate thermal gelation is biologically beneficial. Thermal gelation does not use harsh chemicals or solvents like other hydrogels, which can reduce viability of the incorporated cells. The many types and purities of agarose offer a lot of control over the thermal properties of an agarose mixture, allowing the tuning of the melting and gelling temperatures that are needed for a particular experiment.[32]

Typically, agarose melts at temperatures between 85-95 ˚C and gels around 35-50 ˚C and is dependent on concentration and molecular weight.[48] Low melting agarose was used for this project, which decreases both the melting and gelling temperatures to <50 ˚C and 8-17 ˚C respectively.[48] These lower temperatures are ideal for use with mammalian cells since they cannot be heated above 37 ˚C and premature gelling must be avoiding during the encapsulation process. Another important property of agarose is its thermal hysteresis, where its physical state depends on its thermal history. Once agarose has been gelled, it can be heated up again, past its

gelling temperature, and it will stay in this gelled state at much higher temperatures than before the initial gelling process. Thermal hysteresis is important for this project since agarose must stay liquid at 37 ˚C initially during the encapsulation process, then once gelled, must stay in its gelled state for the therapeutic treatment inside a patient at 37 ˚C.

Agarose has historically been used for a multitude of biomedical applications including use as cell scaffolds[49,50], for tissue engineering to help with cartilage formation, bone regeneration [51], wound healing [52], and encapsulation of cells targeting tumors.[53] Its extensive use with cells highlights its favourable properties, but there are a few disadvantages to using agarose as a cell encapsulation matrix. Agarose does not easily degrade within the human body since there is no available enzyme within mammalian cells; only bacterial cells contain the appropriate enzymes.[54] Keeping the cells encapsulated long-term is beneficial, especially for paracrine effects as continued exposure to secreted factors are beneficial for therapeutic strategies but having agarose microcapsules retained in the body indefinitely is not preferred. One method that researchers have used is to incorporate a degradable hydrogel into the agarose, which has been shown to increase biodegradability.[35] Another issue with encapsulating cells in agarose is that it contains no cell binding domains. However, the structure of the agarose allows for easy chemical modifications, allowing the addition of binding domains, and this approach was used in the present project.

1.7 RGD

Most cell types require adhesion to a substrate to perform their normal functions such as proliferation, migration, and differentiation.[55,56] RGD, the peptide sequence of arginine, glycine,

and aspartate, is the most common cell adhesion domain found within numerous extracellular matrix proteins including fibrinogen, fibronectin, vitronectin and osteopontin.[57] Integrin proteins found within the plasma membrane of all cells, except for red blood cells, bind to this specific amino acid sequence which causes attachment between the cell and its surrounding matrix proteins. Many types of integrins are found on the surface of various cell types and many bind to the RGD sequence making this binding domain non-specific.[58] Therefore, the addition of the RGD sequence onto a hydrogel allows for the attachment of many cell types,. This is an important feature for this research as we would like this technology to be used for many types of cell therapies, using many different cell types.

Recent studies have used this binding domain to modify different hydrogels to increase cell attachment for cell-based therapies. One recent study observed increased osteogenesis with mesenchymal stem cells (MSCs) encapsulated in RGD-modified alginate microcapsules compared to cells mixed with the hydrogel.[59] Another study used human MSCs encapsulated in RGD modified alginate microspheres, to treat myocardial infarction.[60] The results showed increased cell survival for encapsulated cells, but there was no difference in angiogenesis between encapsulated cell treatments and cells alone, even though increased growth factor was observed for encapsulated cell samples. Other studies used RGD modified materials as a bioink for bioprinting purposes.[61] An increase in genes that support chondrocyte formation was observed in one study, in which cells that were encapsulated inside bulk carboxylated agarose functionalized with an RGD peptide.[61] These studies provide insight into cell behaviour with RGD modified materials, but there is not a lot of work investigating the effects of RGD modification on

individual cell laden microcapsules. Most of the RGD modified materials tested in these recent studies used alginate, therefore modifying agarose with RGD sites is of particular interest.

1.8 Cell Types

Most experiments were performed with the NIH 3T3 mouse embryonic cell line. These fibroblast, adherent cells play a critical role in the repair of damaged tissues. Fibroblasts are the most common cell type in connective tissues and are very important in the process of wound healing.[62] They are the least specialized member within the family of connective tissue cell types and are known to secrete high levels of extracellular matrix proteins, specifically type I and III collagen.[62] Because of their enhanced ability to survive in the presence of injury, these cells are very easy to grow in culture. It is also one of the reasons this cell type was chosen for these cell encapsulation studies. Their ease to grow, and their ability to produce extracellular matrix proteins makes them ideal candidates for the early studies of this cell encapsulation project.

Once preliminary data was collected with the NIH 3T3 cell line, more therapeutically relevant cell types were used. Therapeutically relevant cell types are described here as cell types that more closely resemble the cells that will be used for these types of cell-based therapies. Primary cell types are cells that very closely resemble the parental tissue from which they were taken, and they a have much shorter lifespan (usually up to passage 10). Due to their short lifespans and limited time in culture, they show more variability, which is true of real living tissue. Cell lines, like the NIH 3T3 cell line, have been continuously passaged over long time periods and therefore have longer lifespans but have more homogenous phenotypic and genotypic

characteristics. Their homogenous nature means that they are not as biologically relevant, but results obtained with these cells are easier to compare.

The therapeutically relevant cell types used are human umbilical vein endothelial cells (HUVECs), and explant derived cardiac cells (EDCs). HUVECs are an adherent cell type that are very commonly used in research involving endothelial function and diseases. Endothelial cells form the lining of blood vessels and therefore, they control the flow of substances between the circulating blood volume and the surrounding tissues.[63] The endothelium also plays a major role in vasoconstriction and vasodilation, blood clotting and angiogenesis.[63] Since these cells are part of the circulatory system, they are a good model for diseases relating to the heart and blood vessels, which is of heightened interest in this project. Endothelial cells also communicate and initiate many immune responses, including recruitment of immune cells to the site of tissue damage.[64] With the main pathway for cell therapies being paracrine signalling, this communication with immune cells is very important for these studies. Endothelial cells are also known to send signals to the immune system, specifically white blood cells, during inflammatory events,[65] which makes them a great candidate to study paracrine signalling for cell therapies.

EDCs are stem cells extracted directly from myocardial biopsies. They represent a population of heart cells that easily and spontaneously expand in cell culture directly following the removal from patient tissues.[2] There is no arbitrary selection of cells, or prolonged culturing, therefore these grown cells includes many cell populations, including cardiac progenitor cells capable of differentiating into multiple different cell types.[66] Myocardial cells form the majority of the heart and many common heart diseases occur in the myocardium, largely myocardial

infarction. In the United States, one in four deaths are due to heart disease[67], with myocardial infarction occurring in almost 1 million Americans every year[68].

Cell-based therapies have often been used for myocardial infarction due to the limited capacity of heart cells to regenerate.[63] Recent studies have shown that cardiac stem cells (namely EDCs) can provide a beneficial therapeutic effect for injured myocardium when injected into the injured tissues.[1,2] Another important result of these studies with cardiac cells show the limited ability of these injected cells to integrate into the injured tissues with a huge loss of cells during these treatments. Since beneficial effects are still seen with these treatments in repairing tissues damaged from myocardial infarctions, the importance of paracrine signalling of growth factors and cytokine induction are also realized. Initial encapsulation tests with these cardiac cells are critical for the next step of investigating the therapeutic effects of our modified agarose system *in vivo* to further increase the beneficial effects observed with these cardiac therapies.

1.9 Cell-Based Therapies and Their Challenges

Previous research has investigated the use of cell-based strategies to treat tissues damaged from myocardial infarctions.[3,35,69] Effects such as % scar size, change in left ventricular ejection fraction (LVEF) and promotion of angiogenesis during myocardial infarction have

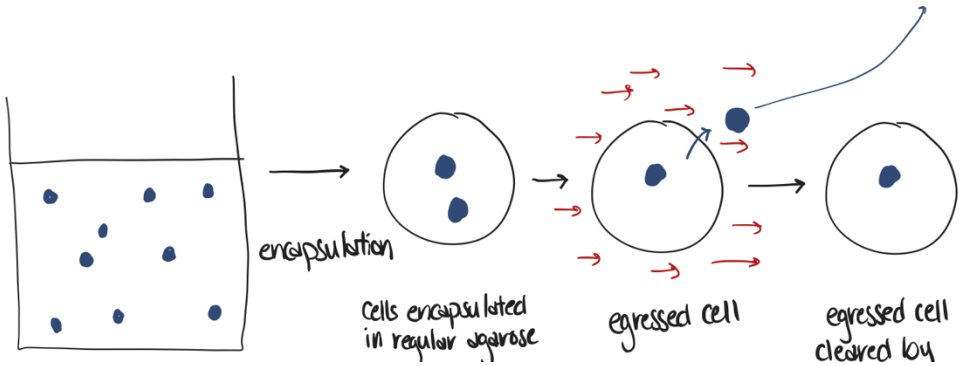

Figure 6 Cells encapsulated in agarose regularly egress or escape from microcapsules. The egressed cells immediately disassociate from microcapsules and are cleared from vasculature and blood flow.

previously been investigated and showed that injections of free cells led to limited therapeutic benefit.[3,69] Recent studies have investigated retention of encapsulated cells and showed progress with this issue by using encapsulated cells, but issues still arose due to cell egress from encapsulation material.[6] Both timepoint images and timelapse video showed that cells can quickly escape (egress) agarose microcapsules quickly following encapsulation.[6] Once egressed, the cells are no longer associated with the agarose microcapsules and therefore become subject to the same clearance as unencapsulated cells.

1.10 Research Outcome

The proposed method of increasing cell retention is by modifying the encapsulation material with cell binding domains, specifically RGD peptides. This modification will reduce cellular clearance following egress from microcapsules. It is hypothesized that the binding sites will provide "grips" or "sticky sites" for cells to bind to the outside of the microcapsule surface once they have egressed from within the microcapsule. By remaining associated with the larger microcapsules, the clearance of egressed cells by fluid flow should be delayed. This should extend the time that these cells remain at the site of injury and continue to impart therapeutic benefit via paracrine signalling.

I set out to achieve three main research outcomes. First, I wanted to determine whether cells would attach to the outside of RGD-modified agarose microcapsules. If indeed they did attach and associate with the RGD-modified material, my next step was to quantify the amount of cellular adhesion occurring for samples of cells encapsulated within this novel biomaterial. The last main objective was to test whether the effects seen with one cell type would transfer to

other cell types, especially more therapeutically relevant cell types that would be used in these cell-based treatments or at least more closely resembled these cell types.

Here I have investigated the behaviour of cells encapsulated in RGD-modified agarose microcapsules and compared that to encapsulation in regular agarose. Using images taken from 2 h to 48 h post encapsulation, I quantified cell viability within the agarose microcapsules, microcapsule occupancy, cell egress from microcapsules, and cell attachment to microcapsules. Using multiple different cell types, ranging in tissue origin, I was able to confirm that multiple cell types do attach to the outside of RGD-modified microcapsules after encapsulation. This novel material does not affect viability of cells encapsulated within RGD-modified agarose microcapsules for up to 48 h, and it does not seem to affect the rate of cell egress from the microcapsules either. Further studies are needed to determine whether this attachment will increase therapeutic effects *in vivo*, but this preliminary work shows promise for reducing cellular clearance at the site of damaged tissue.

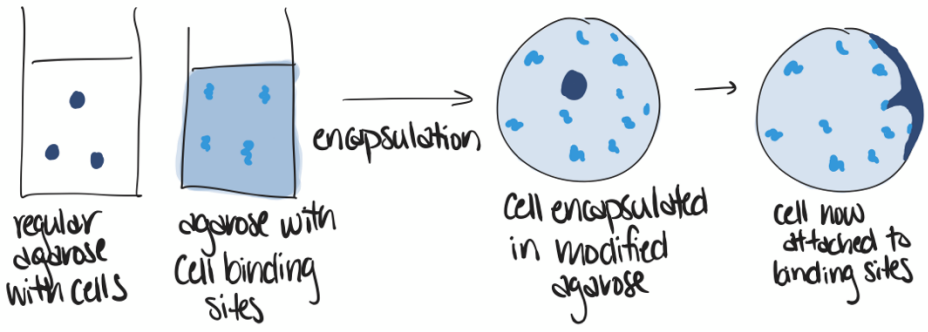

Figure 7 Proposed mechanism of increasing cellular retention by modifying encapsulation material with RGD cell binding domains. Encapsulated cells will still egress from microcapsules, but the binding sites presented on the surface of the microcapsule allow the cell to bind to the outside. This increased association time with the microcapsule will therefore increase cell retention in the injected area.

2 MATERIALS AND METHODS

2.1 Synthesis of Modified Agarose

Agarose was modified to include CRGDS (sequence: CSGSGSGSRGDS) cell binding domains[70]. The addition of RGD onto agarose was completed in two steps. First, agarose was converted into maleimide-agarose using p-maleimidophenyl isocynanate (PMPI). The following reaction was completed under argon: 100 mg of agarose was dissolved in 5 mL of DMSO that was heated to 80 ˚C in an oil bath for 2 h. Once fully dissolved, the agarose solution was cooled to room temperature and 5 mg of PMPI was added to the solution. This solution was stirred overnight at room temperature. This final solution was then dialyzed for 72 h in distilled, autoclaved water, with water exchanged daily. Finally, the dialyzed product was frozen and lyophilized to produce a powder that was then used for the second step of the modification process.

The second step involved attaching CRGDS to the maleimide-agarose product from the last step. The pH of PBS was first adjusted to 6.5-7.5 using dilute HCl, then degassed for 1 h before dissolving the lyophilized maleimide-agarose in the PBS. The PBS was heated to 65 ˚C and then maleimide-agarose was slowly added to make a 2.7% solution of agarose (typically made in batches of 1000 µL). The maleimide-agarose solution was left at 65 ˚C overnight to ensure the agarose was full dissolved. CRGDS peptide was then added to the agarose solution at a concentration of 1.5 mM, which reacted at 37 ˚C for 2 h, under argon. After the reaction, the solution was heated to 60-65 ˚C and aliquoted into smaller vials so that it was not heat repeatedly.

2.2 Soft Lithography Techniques for Wafer Etching

Wafers were used to create the molds used to make poly(dimethylsiloxane) (PDMS) devices. Etching of the devices was completed using standard lithography techniques.[71,72] First, a 100 mm diameter silicon wafer was cleaned from all visible dust and debris through a series of rinsing and drying cycles of acetone, then ethanol, then isopropanol. A second step of plasma cleaning was then conducted by treating the wafer to plasma treatment of 200 W for 10 min to ensure all organic contaminants were removed from the wafer. Next, the wafer must be dehydrated by placing the cleaned wafer on a hotplate at 200 C for 10 min, where it was subsequently cooled for 5 min at room temperature. Next, the wafer was coated with in a 100 µm layer of SU-8 2050 photoresist which is used to create the channel height of my devices. To create the SU-8 layer, a small volume of SU8 2050 was gently poured onto the center of the wafer (approximately 1 mL for every square inch of the silicon wafer). The wafer was then mounted onto a spin coater. The wafer was spun under the following conditions: ramp up to 500 rpm with an acceleration of 100 rpm/s for 10 s, then ramp to 1700 rpm with an acceleration of 399 rpm/s for 30 s, and finally ramp down to 0 rpm with a deceleration of -399 rpm/s. This SU-8 coating was then prebaked at 65 ˚C for 5 min and subjected to a soft bake at 95 ˚C for 16 min, and afterwards cooled for 5 min at room temperature. Next, the SU-8 layer was exposed to UV light which caused a chemical change in the areas exposed to the light. A photomask was placed on top of the SU-8 layer on the wafer, creating a pattern of areas exposed to light and others not exposed. Since SU-8 is a negative photoresist, the areas that were exposed to UV light remained intact once washed

with developer, and the unexposed regions of the SU-8 layer were washed away with a rinse in developer solution.

The wafers were exposed to 230 mJ/cm^2 of UV light to get a height of about 100 µm, therefore the exposure lasted about 15 s. The wafer was allowed to cool for 5 min at room temperature, then baked again at 65 ˚C for 3 min 35 s then to 95 ˚C for 9 min 15 s and finally cooled at room temperature for 5 min. The next step was to develop the SU-8 layer to wash away the unexposed regions of the wafer. The wafer was rinsed in developer for 9 min, while constantly agitating the wafer to ensure the developer flowed over the entire surface. A quick rinse with isopropanol was then completed and the wafer was dried completely using dry nitrogen. The wafer was then placed on a room temperature hot plate and the temperature was set to 150 ˚C so that the wafer would be brought to temperature along with the hot plate. Once 150 ˚C was reached, the wafer was held at this temperature for 5-10 min, then the hot plate was switched off and the wafer was allowed to cool along with the hot plate (covered with a glass dish to ensure it stayed clean). At this point, the preparation of the wafer was complete, and was treated with a silane treatment to increase the durability of the molds for repeated uses.

2.3 Production of Microfluidic Devices

Microfluidic devices were made from polydimethylsiloxane (PDMS; Sylgard 184 Silicone Elastomer Kit, Dow), using the silicon wafer master mold described in the previous section. PDMS was poured on top of the silicon mold at a 10:1 ratio of base to crosslinker. The dissolved air inside the liquid PDMS from mixing was removed by degassing using a vacuum chamber, and then it was cured inside a 70 ˚C oven. The cured PDMS was removed from the wafer using a sharp

blade, cut apart and holes were punched for the inlets and outlets into the PDMS using a skin biopsy punch of 0.75 mm diameter.

Next, PDMS was bonded to glass slides to form functional microfluidic devices. To do this, the PDMS and the cleaned glass slide were plasma treated (Glow Research, AutoGlow System) for 36 s at 36 W. Then, the treated PDMS was placed onto the treated glass slides to allow bonding to occur. To render the PDMS devices hydrophobic, the bonded devices were placed into a 70 ˚C oven. The plasma treatment resulted in hydrophilic devices, but hydrophobicity was needed for the continuous oil phase to flow properly through the device. Finally, the devices were stored at room temperature until use.

2.4 Cell Culturing Methods

All cells were cultured using standard mammalian cell culturing protocols. Briefly, NIH 3T3 cells were cultured in Dulbecco's Modified Eagle Medium (DMEM; VWR), supplemented with 10% fetal bovine serum (FBS; VWR) and 1% penicillin/streptomycin (P/S; Lonza). HUVECs were cultured in endothelial cell media (ECM, ScienCell) supplemented with 10% FBS (ScienCell), 1% endothelial cell growth supplement (ScienCell) and 1% P/S (ScienCell). EDCs were cultured in cardiac explant media (CEM) consisting of Isocove's Modified Dulbecco's Medium (IMDM; Glibco) media supplemented with 10% FBS (VWR), 1% antibiotic-antimycotic (Glibco), 1% l-glutamine (Glibco) and 0.18% β-mercaptoethanol (Glibco). EDCs were grown in fibronectin coated plates.

Cells were subcultured using the ATCC subculturing procedure for NIH 3T3 cells [73]. Briefly, media, PBS, and trypsin (Corning) were warmed to 37 ˚C in a water bath. Cells were grown in 100 cm^2 cell cultured treated petri dishes. Cells were cultured every 2-3 days, when they reached

about 80% confluency in a culture plate. For subculture, media was removed from the cell monolayer, and 5 mL of PBS was then gently added to rinse away remaining media. PBS was then removed, and 3 mL of trypsin was gently added to the plate. Plates were incubated at 37 ˚C for ~3 min to allow cells to detach. Once all cells were disassociated, complete media was gently added to wash and collect the cells. The cell suspension was then centrifuged at 300 x g for 3 min to pellet the cells. Supernatant was removed, and cells were then resuspended in fresh media. The resuspended cells were then added to a new culture plate along with fresh media and placed back in the incubator until the next culture. Other cell types were cultured using the same procedure using appropriate media for each type and TrypLE (Glibco) was used for the therapeutic cell types instead of Trypsin to detach cells from culture dishes. Non-therapeutic cells were cultured between passages 10-30, and therapeutic cells were cultured between passages 2-10.

2.5 Encapsulation of Cells

2.5.1 Encapsulation Setup

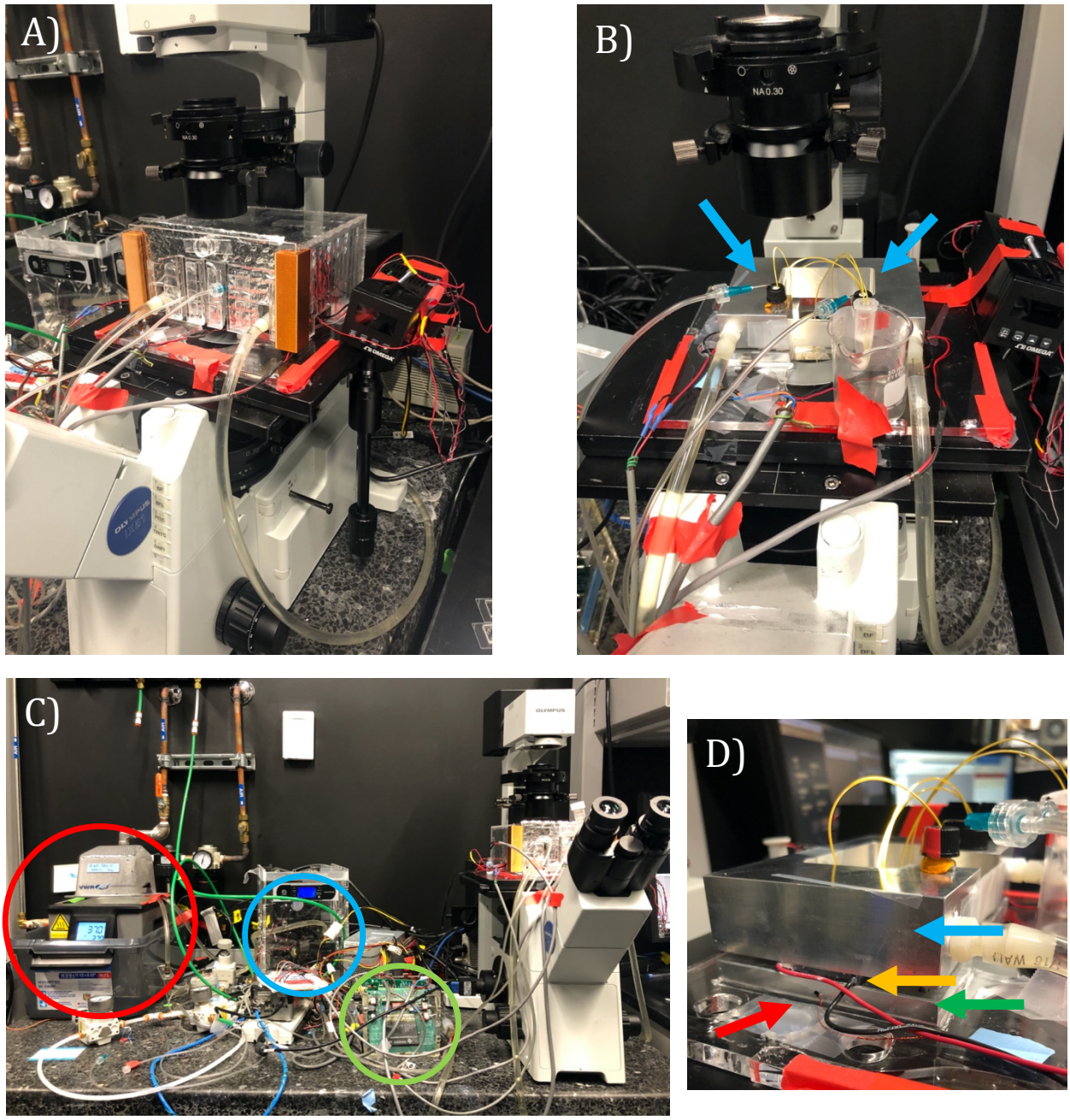

Figure 8 Images of microfluidic encapsulation setup used for experiments.

The equipment used for cell encapsulation used a custom-made microfluidic setup. A microfluidic device was placed underneath a custom-made heatsink and heating/ cooling blocks which all sat

on top of an inverted microscope to allow for visualization of the encapsulation process (Figure 8 B). Water was heated to 37 ˚C using a water bath (Figure 8 C, red circle) and a pump (Figure 8 C, blue circle) pumped this water through tubing connected to the heat sink (Figure 8 D, blue arrow) and through an inner channel within the heatsink and back into the water bath. It was important that the heatsink was heated to 37 ˚C because it contained sample holders for the agarose sample vial and oil vial (Figure 8 B, blue arrows). Since the encapsulation step can take up to 1.5 h, it was very important that the sample was actively heated during encapsulation so that the agarose did not start gelling before the microcapsules were made within the device. The warmer temperature of the heatsink (Figure 8 D, blue arrow) also allowed two Peltier pumps (Figure 8 D, yellow arrow) to transfer heat into the hot block (Figure 8 D, green arrow) and out of the cold block that are located underneath the heatsink and microfluidic device. These hot and cold blocks were used to control the temperature gradient across the microfluidic device. Since the agarose hydrogel used in this project undergoes thermal gelation, controlling the temperature across the microfluidic device was extremely important during the encapsulation process. The left side was maintained at a higher temperature of 37 ˚C to ensure the agarose flowed into the device and microcapsules were made when the agarose was in its liquid state and. The right side was cooled to 4-6 ˚C to gel the newly formed agarose microcapsules as they flowed through the end of the device. The temperature of these blocks was controlled by two Peltier pumps that sat between the heatsink and the hot/cold blocks (shown in Figure 8). The Peltier pumps pumped heat into the hot block from the heatsink to maintain its elevated temperature and pumped heat out of the cold block into the heat sink to maintain its reduced temperature. Thermal paste was used between the Peltier pumps and the heat sink as well as

the hot/ cold blocks to ensure maximal heat transfer between all the components. Thermistors were inserted into holes made within the sides of the hot/ cold blocks (Figure 8 D, green arrow) which were connected to temperature control chips (Wavelength Electronics, HTC3000; Figure 8 C, green circle) that were controlled by custom-made LabView software. This software allowed the user to specify the exact temperature of the aluminum plates that were in direct contact with the Peltier pumps (and therefore the microfluidic device that sat underneath these aluminum plates). The thermistors allowed for a feedback loop to ensure that these blocks were maintained at constant temperatures throughout the entire encapsulation process.

The final major component of the microfluidic setup was the pressure system used to actively flow the fluids (oil and aqueous phases) through the microfluidic device. Pressure regulators were used to precisely control compressed air that was introduced into the system. The compressed air flowed through tubing that was connected to needles that were injected into the sample vials (oil and aqueous phase) to drive the fluids into the connected PEEK tubing that was attached into the microfluidic device (shown in Figure 9). Solenoid valves which were controlled via a custom-made LabVIEW software were used to actuate the pressures within the inlet and outlet tubes. The LabVIEW software allowed control of each individual pressurized unit (oil tubing and aqueous tubing) separately or simultaneous control of all of them.

2.5.2 Microfluidic Device Setup

Cells were encapsulated using a microfluidic device (Figure 9) to produce a high throughput, monodisperse sample of cells within spherical hydrogel microcapsule. Agarose hydrogel and oil phases were driven into the device using pressurized inlets (highlighted section A in Figure 9), forcing the fluids to flow through the device, downstream into the outlets (section

C in Figure 9). Filters were present in all inlets and outlets to ensure that the device was not clogged by large aggregates of cells or microcapsule in the solutions driven through the device. A nozzle, located near the middle of the device, allowed the merging of aqueous and oil flow streams (circle B on Figure 9) and facilitated the formation of agarose microcapsules. The agarose stream was pinched off by the intersecting oil (mineral oil with 1.5% v/v Span 80) streams and an emulsion was created of microcapsules inside the continuous oil phase (Figure 10). Cells were mixed with the liquid agarose hydrogel before entering the device so that the formed agarose microcapsules contained cells. The emulsion then flowed through the serpentine (section D in Figure 9) which is cooled to 4 ˚C to gel the agarose. The serpentine lengthened the time that the agarose was subjected to the cooler temperature to ensure proper gelling of the agarose microcapsules. The emulsion was then collected off chip after exiting the device through the outlets.

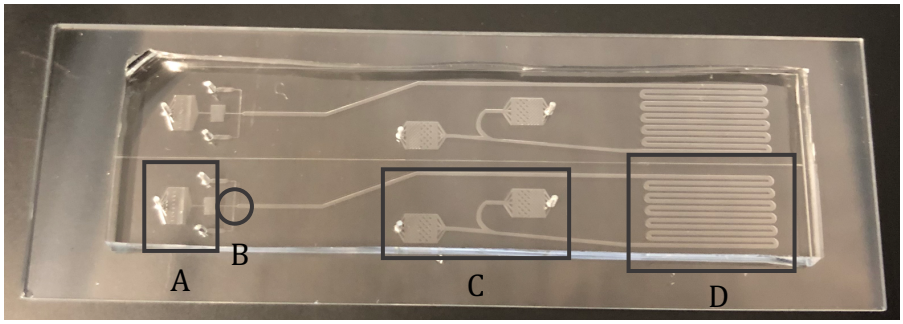

Figure 9 Microfluidic device; PDMS bonded to glass slide. Two devices were bonded to one glass slide. A) inlet holes where agarose and oil were introduced to the device. B) Nozzle where microcapsules were formed and emulsion of microcapsules inside continuous oil phase was created. C) Outlets where the sample exited the device through connected tubing. D) Serpentine where microcapsules were cooled and gelled due to reduced temperature and increased path length.

A heated, insulated acrylic box (Supplementary Information Figure 23) was placed over the encapsulation setup on the microscope stage to keep the sample vials and tubing warm during encapsulation and prevent agarose pre-gelling. This heated box was warmed to 35-36 ˚C and was most important with RGD-modified agarose as this material gels much easier than

regular agarose. Introducing this heated box during encapsulation of RGD-modified agarose resulted in a more monodisperse sample of microcapsules, and no clogging of the microfluidic device, both of which occurred without the use of this box.

2.5.3 Cell Types

Three different cell types were tested using this RGD-modified agarose system - the non-therapeutically relevant cell type of NIH 3T3, as well as therapeutically relevant cell types of human umbilical vein endothelial cells (HUVECs) and explant-derived cardiac cells (EDCs), taken directly from heart tissue biopsies. Different cell types can behave very differently inside these microcapsules based on environmental conditions and stimuli.[6] Therefore, it was important to test this system with multiple different cell types, from different origin tissues, and to investigate their behaviour with our RGD-modified material.

2.5.4 Microcapsule Production

All microcapsules produced were kept at a constant diameter of about 50 µm (52 µm $\pm$ 4 µm) for all experiments. We controlled microcapsule diameter by varying the ratio between the oil and aqueous pressurized inlets to ensure the size was consistent throughout each experiment and between different samples. The number of cells within each microcapsule follows a Poisson distribution and is heavily influenced by microcapsule diameter[23] and therefore it was important to keep this parameter consistent between different experiments as size can greatly affect cell behaviour. Microcapsule size also greatly affects cell egress[6], another parameter we wanted to

keep consistent as we investigated effects of the encapsulation material and cell types on cell behaviour.

For samples of blended RGD-modified and regular agarose, the hydrogel samples were first mixed, and heated to 70 ˚C. For regular agarose samples, the regular agarose was heated first. The sample was slightly cooled at room temperature for about a minute before adding extracellular matrix (ECM) proteins and finally cells immediately before encapsulation. ECM proteins (fibronectin and fibrinogen) were added to the hydrogel to mimic the natural extracellular environment of the cells and to create a more desirable environment. Preparation of the sample directly before encapsulation was important to reduce hydrogel pre-gelling inside the microfluidic device which can cause clogging of this device. The concentrations of components within the final encapsulated sample were: 2% w/v agarose, 8.5 million cells/ mL, 0.1 mg/ mL fibrinogen and 0.1 mg/ mL fibronectin. RGD-modified agarose data included here all used a 2:1 modified to regular agarose ratio as preliminary results show that this material gave the best results in terms of ease of encapsulation and high levels of attached cells.

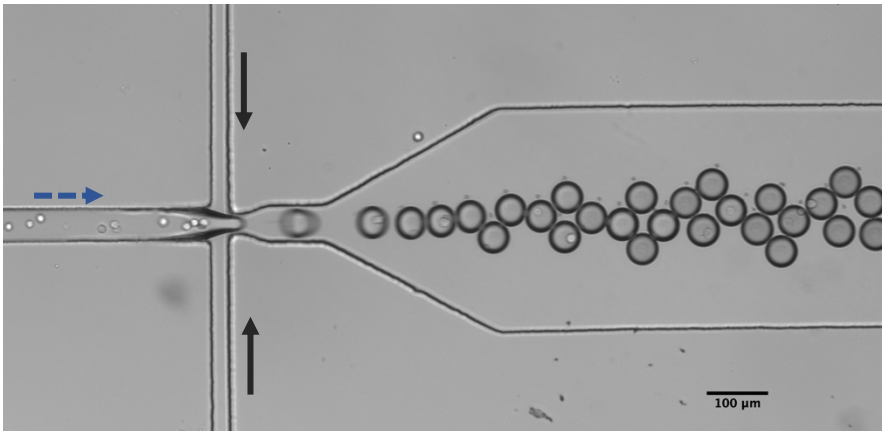

Figure 10 Image of droplet formation at nozzle inside microfluidic device. Full black arrows show flow of continuous/ oil phase. The blue dashed arrow shows the flow of dispersed, aqueous flow. Cells are seen inside the aqueous agarose stream, and within the monodisperse microcapsules formed downstream of nozzle.

Images of microcapsules made within the microfluidic device were taken throughout the encapsulation process (Figure 10) and diameters were measured using ImageJ. Inlet pressures were altered accordingly to maintain 50 µm diameter microcapsules. Approximate pressures used were approximately 0.11 MPa for oil inlets and 0.12 MPa for the agarose inlet, using the microfluidic device shown in Figure 9. With these pressures, a typical 150 µL sample took about 1 h 20 min to encapsulate.

2.5.5 Mixing Experiments

Mixing experiments were also conducting using empty microcapsules, i.e., no cells inside. These empty microcapsules were made using the same method described above except that no cells were present, and PBS was used to make up for the missing volume in the agarose solution. Microcapsules were made using this solution inside the microfluidic devices and were collected in media. Cells suspended in media were then mixed with the empty microcapsules in media to investigate the attachment of non-encapsulated cells to different agarose types. The same method was used for analysis for both encapsulated cells and mixed cell samples.

2.6 Preparation of Samples

After microfluidic encapsulation, microcapsules were collected into a centrifuge tube filled with 500 µL of media, kept on ice. Separation of the top oil phase and the bottom aqueous phase containing microcapsules was first done following centrifugation. The sample was centrifuged two times at 3 min at 300 x g, with the sample transferred into a new tube between each centrifugation step. Transferring of the sample helped to remove all traces of oil present in

the aqueous phase. Samples were then prepared for two separate analysis methods – timepoint microscopy studies and Cell Counting Kit-8 (CCK-8) studies. Timepoint microscopy samples were prepared in 35 mm cell culture treated petri dishes, containing 70-100 µL of microcapsule sample and 1000 µL media. Six samples were prepared for each experiment, 3 timepoints (2 h, 24 h, and 48 h after encapsulation) with two different dish coating conditions. One set of samples had no dish coating so that cells could adhere to the dishes surface, and the other set consisted of dishes coated in poly(2-hydroxyethyl methacrylate) (pHEMA). The pHEMA coating eliminated cell adhesion to the Petri dish, thereby mimicking an environment where no nearby surface was available for the attachment of egressed cells. All samples measured using CCK-8 studies were completed in pHEMA coated 96-well plates. A schematic of the entire sample preparation procedure is shown below (Figure 11).

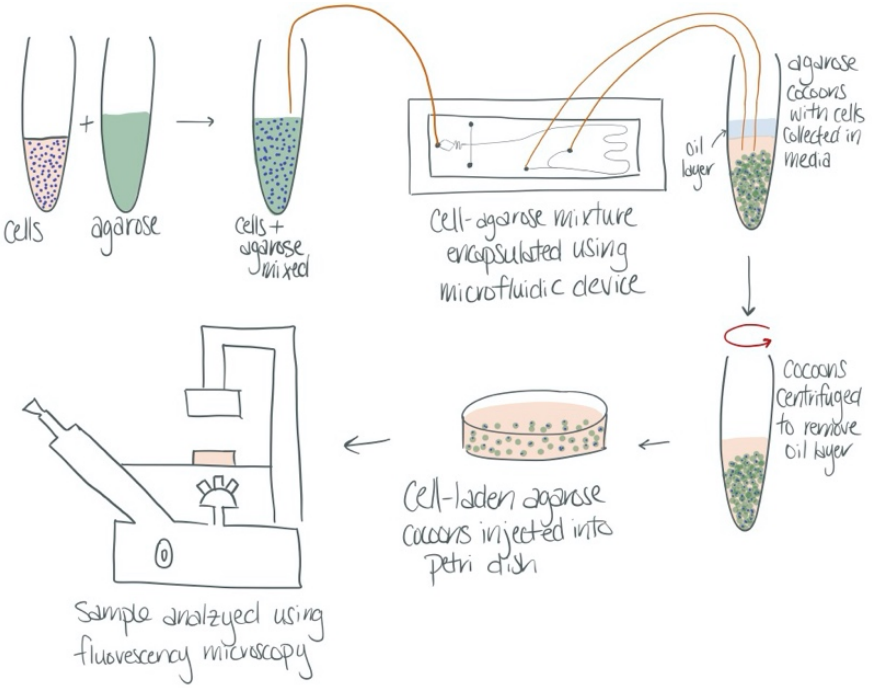

Figure 11 Schematic of experiments. Cells and agarose were mixed together, then used in the microfluidic device to create cell-laden microcapsules. After encapsulation, the sample was centrifuged to easily remove all oil from sample. The purified sample was then added to petri dishes to conduct timepoint analysis of each sample using a fluorescence microscope.

2.7 Timepoint Analysis

Samples were analyzed at three timepoints (2 h, 24 h, 48 h) to track cell behaviour in the agarose microcapsules. The first timepoint (2 h) was the earliest possible time to analyze the sample. Encapsulation typically took about 1.5 h to complete, and the viability assay must sit at room temperature for 30 min before imaging. Therefore, the 2 h timepoint was used as the initial sample and many quantities were referenced from the data collected at this time.

Images were collected at each timepoint and allowed for measurements of cell viability. Cells were first stained using a fluorescence viability stain (LIVE/DEAD Viability/ Cytotoxicty kit, Invitrogen). The stain was comprised of calcein (1.2 µM) and ethidium homodimer-1 (EthD-1; 1 µM) in PBS and 0.25-0.5 mL of this solution was added to each sample. These dishes were held at room temperature for 30 min before imaging on an Olympus IX51 fluorescence microscope using a FITC filter for calcein and a TRITC filter for EthD-1. Each analyzed image consisted of three separate images – a FITC image, a TRITC image and a brightfield image to view the agarose microcapsules (example images shown in Supplementary Information Figure 22). The brightness and contrast of each image was optimized, and the three images were compiled together in ImageJ, to then be used for analysis.

Analysis of each image was completed by manually counting microcapsules, noting the number of cells inside, and cells were categorized as either dead (red cells) or alive (green cells), due to fluorescence staining from the Live/Dead kit. Five images of each sample were collected at each timepoint to use for analysis. The images collected for viability studies were also used to

measure other quantities, specifically microcapsule occupancy, cell egress/ escape from microcapsules, and cell attachment to microcapsules.

2.7.1 Cell Egress

Egress is defined as the fraction of encapsulated cells that migrate out of the hydrogel microcapsules. It is determined using the change in occupancy of the microcapsules between the various timepoints, using the following equations:

$$\%\ \text{cumulative egress} = \frac{\text{occupancy}_{2\text{h}} - \text{occupancy}_{24/48\text{h}}}{\text{occupancy}_{2\text{h}}} \tag{5}$$

$$\text{occupancy} = \frac{\#\ \text{total encapsulated cells}}{\#\ \text{total microcapsules}} \tag{6}$$

The subscript values refer to the timepoint for each image. Equation 5 was used for either the 24 or 48 h timepoint and both calculations were referenced with respect to the initial 2 h timepoint, as cumulative egress was calculated here.

2.7.2 Viability

Viability was determined using the number of live and dead cells. Any egressed cells at later timepoints were considered to be alive; therefore, live cells were defined as all live encapsulated and all egressed cells in the images. Total cells referred to all cells, regardless of whether they were encapsulated or not. The following equation was used to calculate cell viability:

$$\%\ \text{viability} = \frac{\#\ \text{live cells}}{\#\ \text{total cells}}. \tag{7}$$

2.7.3 Cell Attachment

Attached cells were identified by irregular cell shapes that contoured around the edge of agarose microcapsules; examples are shown in Figure 17. Cell shape was not always easy to determine, due to some cells lying outside the focal plane, therefore inherit variability was present when determining this quantity. Cell attachment was calculated using the number of egressed cells that then attach to the outside of microcapsules, using the following equation:

$$\%\ \text{cells attached} = \frac{\#\ \text{attached cells}/_{\text{microcapsule}}}{\#\ \text{egressed cells}/_{\text{microcapsule}}} \tag{8}$$

where

$$\#\ \text{attached cells}/_{\text{microcapsule}} = \frac{\#\ \text{attached cells}_{24/48\text{h}}}{\#\ \text{total microcapsules}_{24/48\text{h}}} \tag{9}$$

and

$$\#\ \text{egressed cells}/_{\text{microcapsule}} = \frac{\#\ \text{live encap. cells}_{2\text{h}} \times\ \%\ \text{cumulative egress}_{24/48\text{h}}}{\#\ \text{total microcapsules}_{2\text{h}}}. \tag{10}$$

As with Equation 5 for cumulative egress, the subscripts 2h, 24h, and 48 h refer to the timepoints for each image. Equations 8-10 were used for both 24 h and 48 h timepoints with the corresponding data used for the calculations of the number of attached and egressed cells for each timepoint.

2.8 CCK-8 Studies

Cell viability was also determined using a second method to achieve a deeper understanding of the health of the cells. CCK-8 studies measure the number of metabolically active cells in the sample. All CCK-8 samples were prepared in 96 well plates, all with the pHEMA dish coating. The CCK-8 reagent was added to each sample 2 h before the absorbance reading using a plate reader. A calibration curve using a range of different cell concentrations was completed for each cell type and was used to convert absorbance readings of each sample to the number of metabolically active cells in the sample.

2.9 Confocal Microscopy of Focal Adhesions

The presence of focal adhesions on encapsulated and egressed cells was investigated using a staining protocol for actin cytoskeleton and vinculin. Cell samples were stained according to the protocol described for the Actin Cytoskeleton and Focal Adhesion kit (Millipore) that was used. Briefly, encapsulated cell samples were first prepared by gently centrifuging encapsulated cells suspended in media for 5 min at 300 x g. Once a pellet was formed, the supernatant was carefully removed, leaving as little remaining media as possible. PBS was then added, the sample resuspended, and then centrifuged again under the same conditions to pellet and remove PBS. Due to the nature of these samples, and the fact that the cells were not attached to a glass slide, but free floating in microcapsules in a solution of media, all washing steps were conducting using this protocol of centrifugation, resuspension in PBS, then centrifugation again to remove PBS. Next, encapsulated cells were fixed using a 4% (w/v) paraformaldehyde solution in PBS for 20 min at room temperature with mild shaking. Encapsulated cells were washed twice with PBS,

then permeabilized with a solution of 0.1% (v/v) Triton X-100 in PBS for 5 min at room temperature. The sample was again washed twice with PBS as previously described. The encapsulated cell pellet was then blocked using a blocking solution of 1% (w/v) BSA in PBS for 30 min at room temperature. Anti-vinculin antibody (1:500 v/v in blocking buffer) was then added to the sample and incubated at room temperature for 1 h with mild shaking. The sample was then washed twice with PBS and an anti-mouse-Alexaflor 488 (ThermoFisher) was used at a 1:1000 dilution in blocking buffer to tag the anti-vinculin antibody for visualization. Simultaneously, TRITC-conjugated to Phaloidin was added to the blocking buffer (1:1000 v/v) to visualize the actin cytoskeleton. For the last 5 min of the staining procedure, DAPI was added to the staining buffer to label cellular nuclei. A final wash with PBS was performed to remove excess stain. Encapsulated cells were placed onto glass slides and covered with glass coverslips. Cover slips were sealed, and slides were cleaned for observation. Confocal microscopy was conducting using a Ziess LSM 880 confocal microscope. Carl Zeiss ZEN 2.3 (black; release version 13.0.0) software was used to edit and analyze the images.

2.10 Statistical Analysis Methods

All statistical analysis was completed using Excel and R software. All tests between different timepoints (same agarose types and plate coatings) were conducted using paired T tests, and all others comparing agarose types and plate coating conditions for the same time point were conducted using Student T tests. All graphs show error bars of standard error of the mean.

3 RESULTS AND DISCUSSION

The research presented here describes one proposed method of increasing cell retention in cell-based therapeutic strategies. One common issue with these cell strategies is the low retention of cells at the site of interest due to negative immune responses and vasculature clearance. Without cells near the injured site for long periods of time, these cells cannot impart strong paracrine signalling, or engraft into the damaged tissue. This loss of cells leads to reduced efficacy of cell-based treatments. Encapsulation of cells in hydrogel microcapsules has been shown to increase the retention of cells at the injection site[3], but other studies have shown that cells can still egress agarose microcapsules very quickly.[6] Cell egress limits the beneficial effects of encapsulation because the cells escape the microcapsules and dissociate from the hydrogel immediately, which means that negative immune effects and vasculature clearance are once again affecting these cells and clearing them from the site.

The proposed strategy for increasing cellular retention is through modifying the encapsulation hydrogel with cell binding domains, specifically RGD sites. The addition of cell binding domains allows the cells to attach to the outside of the microcapsule once it has egressed, and therefore allows for longer association with the microcapsule. Longer association time is hypothesized to increase the efficacy of these cell treatments due to a longer time to provide paracrine signalling or allow more time to engraft into surrounding tissues.

The attachment of cells onto RGD-modified agarose microcapsules was investigated by encapsulating cells in RGD-modified agarose microcapsules and comparing their behaviour to cells encapsulated in regular agarose microcapsules. Cell behaviour was determined using

timepoint fluorescence images to study cellular egress from the microcapsules and the viability of the cells inside and outside the microcapsules, and to observe and quantify cell attachment to microcapsules. Encapsulated cells were observed at three timepoints after encapsulation and these quantities were compared to identify changes to cell behaviour with time. These experiments were conducted in different cellular environments used to mimic different *in vivo* conditions and using multiple cell types to determine whether the effects observed with RGD-modified agarose was cell specific or can be used in the future for multiple different cell-based strategies with many different targeting tissues.

3.1 Encapsulation of Cells

Cells were encapsulated in both regular agarose and RGD-modified agarose using a microfluidic approach to compare these two different materials. Encapsulation using RGD-modified agarose was more challenging than regular agarose as the physical properties of the agarose changed due to the RGD modification. The melting and gelling temperatures shifted and therefore higher temperatures were needed to keep the RGD-modified agarose in its fluid state, which was difficult during encapsulation since the temperature of the cells could not be raised above 37 ˚C. RGD-modified agarose was melted at 70 ˚C, whereas regular agarose was routinely

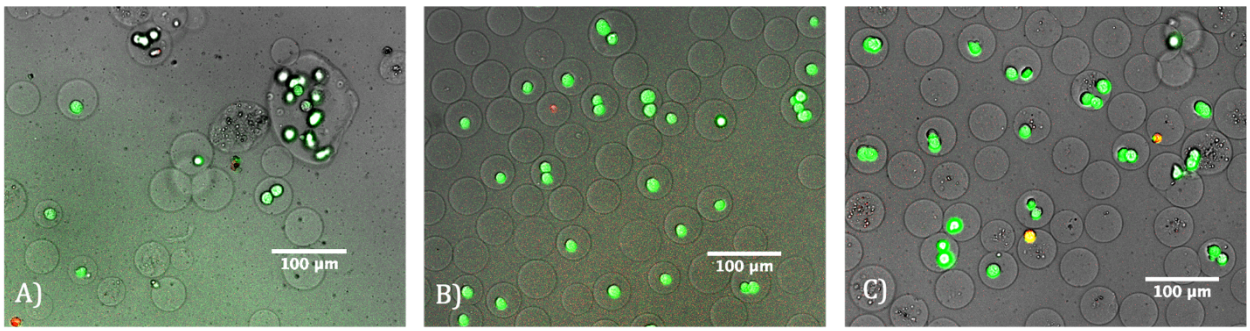

Figure 12 NIH 3T3 cells encapsulated in A) 100% RGD-modified agarose, B) 100% regular agarose, C) 2:1 RGD-modified to regular agarose blend. The blended sample clearly shows microcapsule size and shapes that are more similar to regular agarose than 100% RGD-modified agarose.

melted at 60˚C, with a noticeable change in the fluid state of the RGD-modified agarose inside the tube at this higher temperature. When vortexing the melted RGD-modified agarose solution, the meniscus did not move up the side of the tube at 60 ˚C, whereas at 70 ˚C the meniscus was seen very easily moving up the side of tube during vortexing. Microcapsule formation using 100% RGD-modified agarose created "messy" samples - microcapsules were misshapen, inconsistently sized (as shown in Figure 12 A) and the agarose often clogged the microfluidic device due to pre-gelling in the inlet. NIH 3T3s encapsulated in regular agarose microcapsules are shown in Figure 12 B, where microcapsules have very uniform sizes and shapes, with cells evenly distributed between the microcapsules, and no agarose clumps were present. For this reason, a blend of regular and RGD-modified agarose was used for experiments as this helped keep the agarose in its fluid state within the required temperature range. Eventually a blend of 2:1 modified to regular agarose was chosen due to ease of encapsulation within the microfluidic device, and increased viability compared to full modified agarose. NIH 3T3s encapsulated in this 2:1 RGD-modified to regular agarose blend are shown in Figure 12 C, where it can be clearly seen that the size and shape of microcapsules was more similar to that of regular agarose sample (Figure 12 B). This dilution of RGD-modified agarose gave a concentration of RGD sites in the final solution used for encapsulation (assuming homogeneous distribution of RGD sites) of about 3×10^8 RGD sites/ pL, which is roughly 2×10^{10} RGD sites/ droplet, or a surface concentration of roughly 4500 RGD sites/μm^2 , which should be sufficiently concentrated for cells to easily find RGD sites in the diluted encapsulation material if desired.

Timepoint images of cells encapsulated in regular agarose microcapsules clearly showed signs of cell escape or egress from the microcapsules. Figure 13 shows images of NIH 3T3 cells

encapsulated in regular agarose at A) 2 h after encapsulation, and B) 48 h after encapsulation. At 2 h, the cells were clearly all encapsulated inside the agarose microcapsules, and were in their rounded, unattached state inside the hydrogel matrix. After 48 h, the NIH 3T3 cells have escaped the hydrogel, and have attached to the bottom of the culture dish in which the sample was incubated, highlighted by red arrows in Figure 13 B.

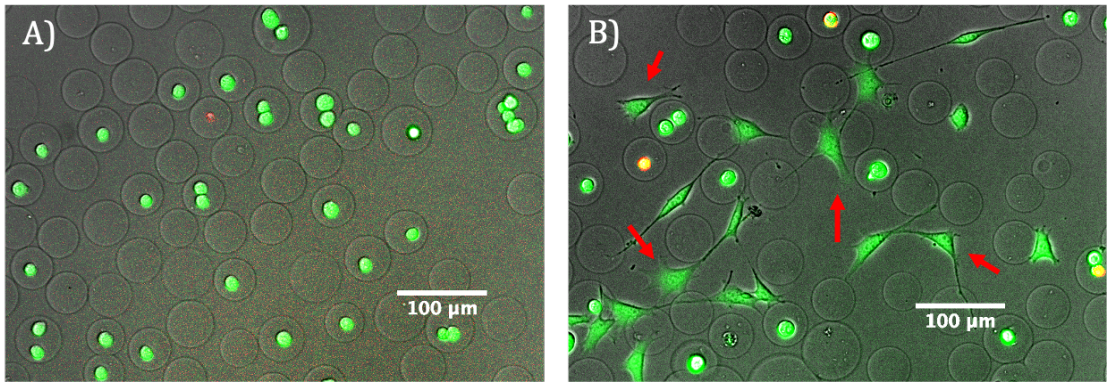

Figure 13 NIH 3T3 cells encapsulated in regular agarose at A) 2 h and B) 48 h after encapsulation. Sample incubated in regular dish coating. Cells have escaped the agarose microcapsules and are seen attached to the bottom of the dish after 48 h, whereas all cells are encapsulated at 2 h. Red arrows highlight cells that have egressed and attached to bottom of dish.

One of the main reasons that cells are encapsulated in hydrogels for cell-based treatments is to reduce cellular clearance at the site of injury. The increased size of the hydrogel spheres reduces the clearance of the much smaller cells inside the hydrogel, since the fluids flowing through tissues cannot easily move these hydrogels. Cell egress from agarose microcapsules reduces these beneficial effects of encapsulation since egressed cells are once again free floating and therefore can easily be cleared from the injection site. Cellular egress must be reduced to obtain high levels of injected cells at the site of injury. In this study, the percentage of cells lost from egress was quantified and allowed for the determination of any effects on cell behaviour due to the RGD-modification of the agarose.

3.2 Microcapsule Occupancy

Microcapsule occupancy (Equation 6) was used to determine cell egress from the microcapsules. As shown in Figure 14, occupancy mostly decreased for each sample with time, due to cell egress, which was expected from previously published research.[6] These results also confirmed that most of the cell egress was occurring in the first few hours after encapsulation, as seen by the largest decreases in microcapsule occupancy between the 2 h and 24 h samples, specifically for the NIH 3T3s in regular agarose, HUVECs in regular agarose, and EDCs in RGD-modified agarose.

The variability in the cell egress values was quite large, most likely due to sample preparation methods. The cell concentration in the liquid agarose solution used for encapsulation most directly affected the determination of the initial microcapsule occupancy, and issues with cells clumping prematurely, and any inaccuracies in cell counting can also lead to drastic effects on cell concentration and therefore the initial microcapsule occupancy. Chilling the cells before use and counting multiple aliquots of the cell solution helped to decrease this variability but, to some degree, it is unavoidable during these experiments.

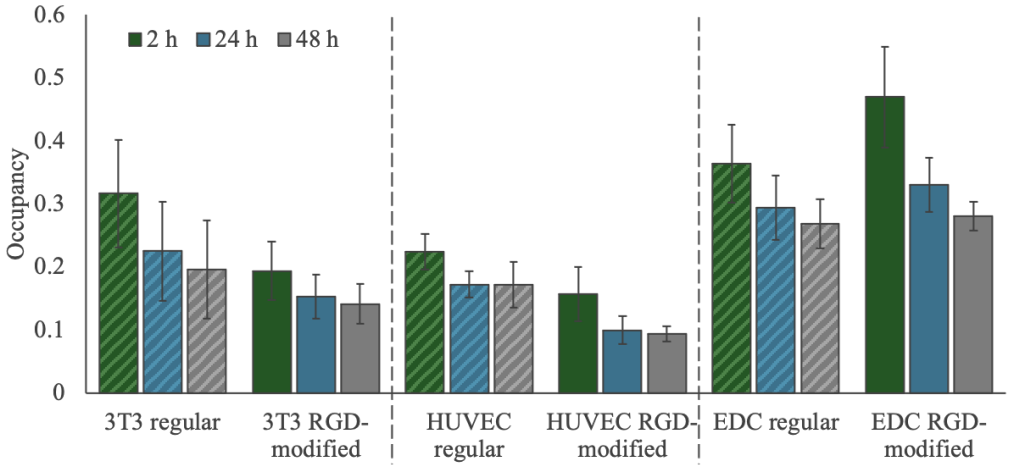

Figure 14 Occupancy data of microcapsules for different cell types at three different timepoints after encapsulation. Data shown here was collected from cell culture treated plates. Shown is mean ± SEM. $n \geq 3$ for each data point.

3.3 Cell Egress

Early results indicated that cells egress regular agarose microcapsules quickly and effectively after encapsulation, as shown in Figure 15. In fact, 40% of NIH 3T3 cells encapsulated in regular agarose egress within 48 h. For the therapeutic cell types tested (HUVEC and EDC), egress efficiency is slightly reduced, with about 25% cell egress (24% and 25% respectively) after 48 h in regular agarose. Results for RGD-modified agarose do not show significant differences in cell egress efficiency compared to those measured for regular agarose.

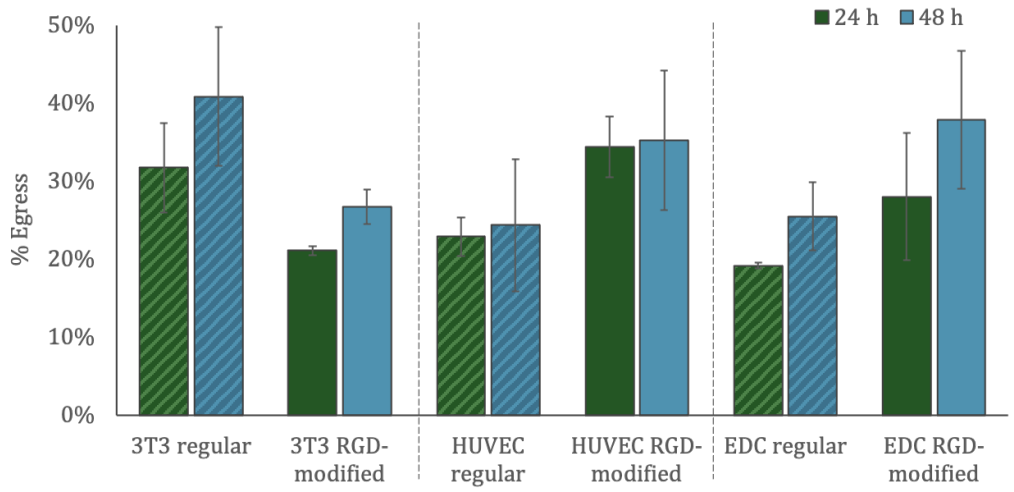

Figure 15 Plot of cell egress with three cell types. Data collected on regular dish coating surface. Striped bars show data collected with regular agarose, and solid bars show data collected with RGD-modified agarose. $n \geq 3$ for all data points. Shown is mean ± SEM. * $p < 0.05$ using t tests for comparisons of different agarose types.

These results are relatively consistent with previous research where observed cell egress from regular agarose microcapsules was about 25% for NIH 3T3s and 30% for HUVECs, 48 h post encapsulation.[6] The results provided here correspond to values of 40% for NIH 3T3s and 25% HUVECs with the same experimental conditions. Possible changes in gelling time in the present study may account for the slight differences in cell egress, especially with the NIH 3T3 cells. The

heated box used in these experiments may have led to increased gelling time and therefore affected cell egress from microcapsules.

3.4 Cell Viability

Previous studies on microfluidic encapsulation of cells showed that the encapsulation process used here does not have a negative effect on cell viability.[3,6] In the present study (Figure 17), cell viabilities were quantified post encapsulation at a 2 h timepoint. NIH 3T3 cells showed viability at this timepoint of (97 $\pm$ 1)% and (75 $\pm$ 3)%, HUVECs with (94 $\pm$ 1)% and (84 $\pm$3)%, and EDCs with (95 $\pm$ 1)% and (76 $\pm$ 3)%, for regular agarose and RGD-modified agarose respectively. NIH 3T3s encapsulated in regular agarose showed statistically no change in viability over 48 h, whereas the HUVEC and EDC cells showed a significant reduction in cell viability. There are no statistical changes in viability between agarose types at the later timepoints of 24 h and 48 h. Differences were observed at 2 h for NIH 3T3s and EDCs. There was a decrease in viability of EDCs in regular agarose with time (95 $\pm$ 1)% at 2 h, (64 $\pm$ 4)% at 24 h, and (54 $\pm$ 7)% after 48 h. No statistical difference was observed in viability with time for NIH 3T3s and HUVECs in regular or RGD-modified agarose.

The high values of initial cell viability indicate that the encapsulation process and sample preparation was not exceptionally stressful for the cells, consistent with our previous findings[3,6]. Viability differences between agarose types at the initial timepoint could be due to differences in sample preparation, or the passage number of the cells. Since the later timepoints showed no significant differences, and these initial differences were not seen for all cell types, it was most likely not the agarose type that caused these differences.

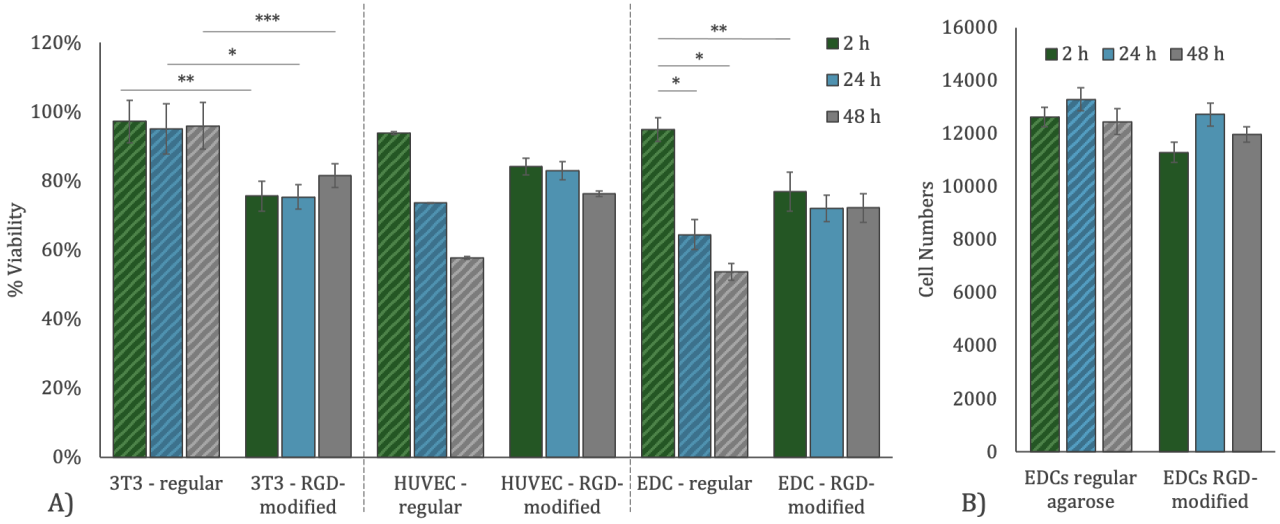

Figure 16 Plot of cell viability, for samples on pHEMA coated dishes. Striped bars show data collected with regular agarose; solid bars show data collected with RGD-modified agarose. A) Viability determined through live/dead fluorescence assay. B) CCK8 results for EDC samples. $n \geq 3$ for all samples. Shown is mean ± SEM. * $p < 0.05$, ** $p < 0.01$, *** $p < 0.001$ using paired t test for comparisons between different timepoints, t tests for comparisons between different agarose types.

Initial occupancy values were slightly lower with EDCs encapsulated in regular agarose compared to the RGD-modified samples (36% versus 47% occupancy, respectively; Figure 14), which could lead to the lower viability observed for the EDC samples. Cell behaviour is heavily influenced on proximity to nearby cells[3]; therefore, lower occupancy means less cells nearby each other that potentially decreased viability. Another reason for this could be that primary cells are more affected by environmental conditions, and therefore effects are greater with EDCs than with a cell line like NIH 3T3s.

Cell viability was also assessed through a CCK-8 proliferation assay (Figure 16 B). Two methods were used to quantify cell viability because each method assesses different characteristics of cell viability. The live/dead fluorescence assay measures the membrane integrity of the cells as well as intracellular esterase enzymatic activity.[74] The CCK-8 assay measures the amount of solute added to a cell solution that is converted into a visible product through intracellular transport of electrons.[75] Therefore, this assay quantifies the number of cells

that are undergoing regular intracellular activities. Both assays are regularly used to quantify cell numbers and viability in cell samples.[3,6,59] Quantifying metabolically active cells as well as quantifying cell membrane integrity are crucial factors to ensure cell survival; therefore, it was important to investigate both properties.

We assessed encapsulated EDC cells using a CCK-8 assay. The CCK-8 results showed that EDCs had no significant change in cell viability/ proliferation up to 48 h after encapsulation in either agarose type. In Figure 16 B, we can see that all results corresponded to statistically the same number of cells at all three timepoints (12600 $\pm$ 400 cells and 12500 $\pm$ 500 cells for regular agarose at 2 h and 48 h timepoints respectively, and 11300 $\pm$ 400 and 12000 $\pm$ 300 cells for RGD-modified agarose at 2 h and 48 h timepoints respectively). This is a different trend than the results for EDCs encapsulated in regular agarose using the fluorescence viability assay. There are a few possible reasons for this apparent contradiction. The sample size measured using the CCK-8 assay reflects the entire sample in the dish, which is much larger than the manual counting of cells from a small subsample of the dish with the fluorescence viability assay. The smaller sample will inherently have more variability in the measured quantity. The microcapsule concentration inside the dishes was also much higher for the CCK-8 assay compared to the fluorescence assay to ensure the absorbance signal lay within the optimal, linear region of the calibration curve. Due to the high concentration, egressed cells must be much closer to each other, which could have led to cell clumping and some proliferation outside the microcapsules and therefore an increased signal.

The CCK-8 assay also revealed that using RGD-modified agarose did not significantly reduce the metabolic activity of encapsulated EDC cells. These tests were conducted in stationary

samples, where all cells in the initial sample remained within the well for the duration of the test. In an *in vivo* environment, many of the egressed cells that do not attach to a microcapsule are quickly cleared away from the targeted tissue via vasculature flow.[3]

3.5 Cell Attachment to Microcapsules

Previous *in vivo* studies suggested that agarose microcapsules tend to remain in the targetted tissue for days, whereas cells that egress these microcapsules are quickly cleared out of the tissue by vasculature.[3] Cells encapsulated in RGD-modified agarose also egress their microcapsules, as shown above in Figure 17, but these cells are observed to adhere to the outside of these microcapsules. Examples of encapsulated cells are shown below, in RGD-modified agarose in Figures 17 and in regular agarose in Figure 18, all shown 48 h post encapsulation, in pHEMA coated dishes. Each image in Figure 17 shows cells that have egressed their microcapsule and were now clearly wrapping around the microcapsule surface. Red arrows highlight the cells that are identified as attached to the RGD-modified agarose microcapsules. Figure 17 A shows EDCs encapsulated in RGD-modified agarose and Figure 17 B-D shows NIH 3T3s encapsulated in RGD-modified agarose. As can be seen in these images, various cell shapes and conformations were observed in samples of cells encapsulated in RGD-modified agarose. Small clumps of attached cells were common, as shown in Figure 17 D, as well as cells lying in between multiple microcapsules, as shown in the bottom aggregate of cells of Figure 17 C.

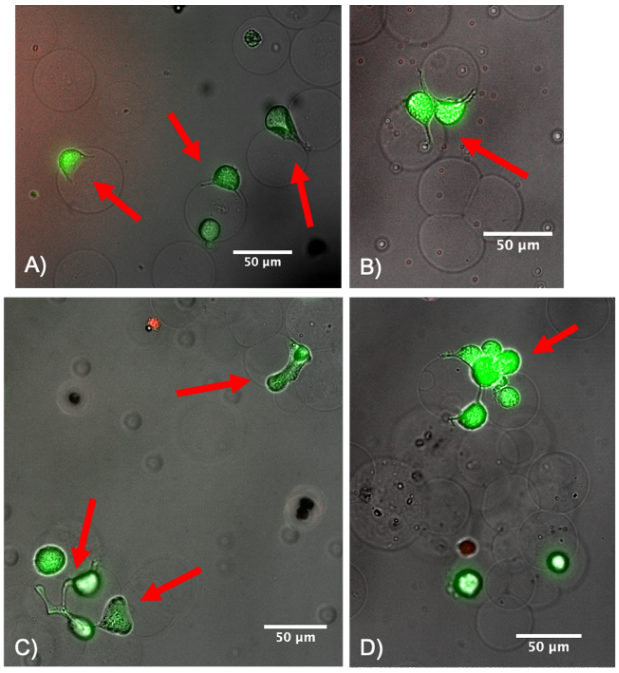

Figure 17 Cells encapsulated in RGD-modified agarose microcapsules. All red arrows highlight cells that are attached to microcapsule surfaces. A) EDCs after 48 h in pHEMA coated dish B), C), D) all show NIH 3T3s after 48 h in pHEMA coated dishes. Various examples of shapes of cells can be seen attached to the outer microcapsule surfaces.

In contrast, cells encapsulated in regular agarose showed essentially no indication of cell attachment, or any wrapping around the outside of microcapsules, as shown in Figure 18. EDCs encapsulated in regular agarose are shown in Figure 18 A, and NIH 3T3s encapsulated in regular agarose are shown in Figure 18 B. The red arrows highlight cells that have egressed the microcapsules, but remained rounded and spherical in shape, without any apparent associations with the regular agarose microcapsules. These reference samples highlight the drastic difference in cell behaviour and shape observed between cells and RGD-modified agarose material and cells regular agarose material.

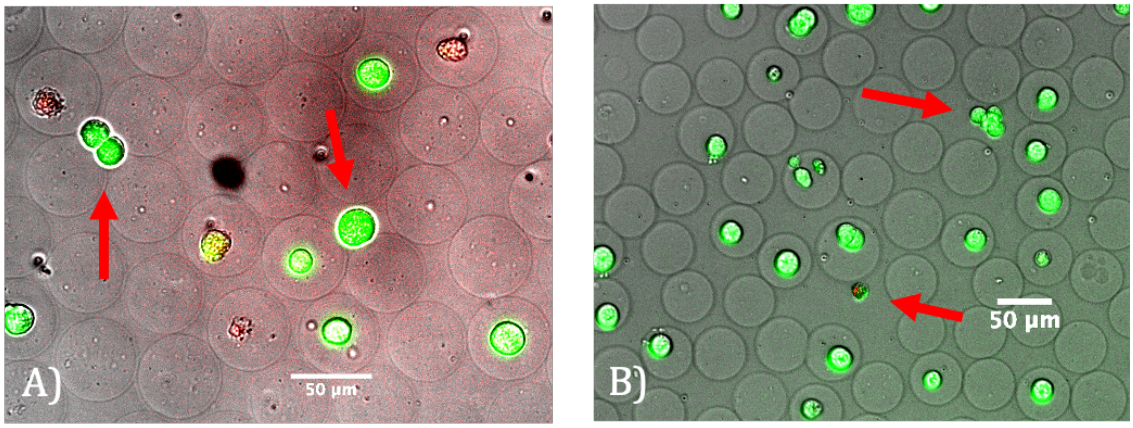

Figure 18 Cells encapsulated in regular agarose. All red arrows show egressed cells that are not attached to surface. A) EDCs after 48 h in pHEMA coated dish B) NIH 3T3s after 48 h in pHEMA coated dish. All egressed cells are seen in rounded, unattached state.

Cell attachment to RGD-agarose microcapsules was observed for all cell types tested, for both plate coatings of regular culture treated dishes, as shown in Figure 19 A, and adhesion inhibited coatings with pHEMA, as shown in Figure 19 B. NIH 3T3s presented the highest level of attachment with around 40% of the egressed cells attached to microcapsules after 24 h, as observed on pHEMA coated dishes. There was nearly no cell attachment to regular agarose microcapsules under all sample conditions – less than 5% cell attachment for all cell types, plating conditions, and timepoints. Meanwhile RGD-modified agarose microcapsules had up to 43% attached NIH 3T3s, 33% attached HUVECs, 20% attached EDCs, as shown in Figure 19. EDC cell attachment also improved with pHEMA coated plates compared to no coating: (3 ± 1)% and (16 ± 1)% after 24 h, and (1 ± 1)% and (20 ± 3)% 48 h, for uncoated and pHEMA coated plates respectively. Since regular dish coating is optimized for cell attachment, these results suggest that therapeutic cells have increased attachment to RGD-modified agarose microcapsules when

no other optimal surface for attachment is available in their surroundings. In pHEMA coated dishes, we observed the cells wrapping themselves around the RGD-modified microcapsules.

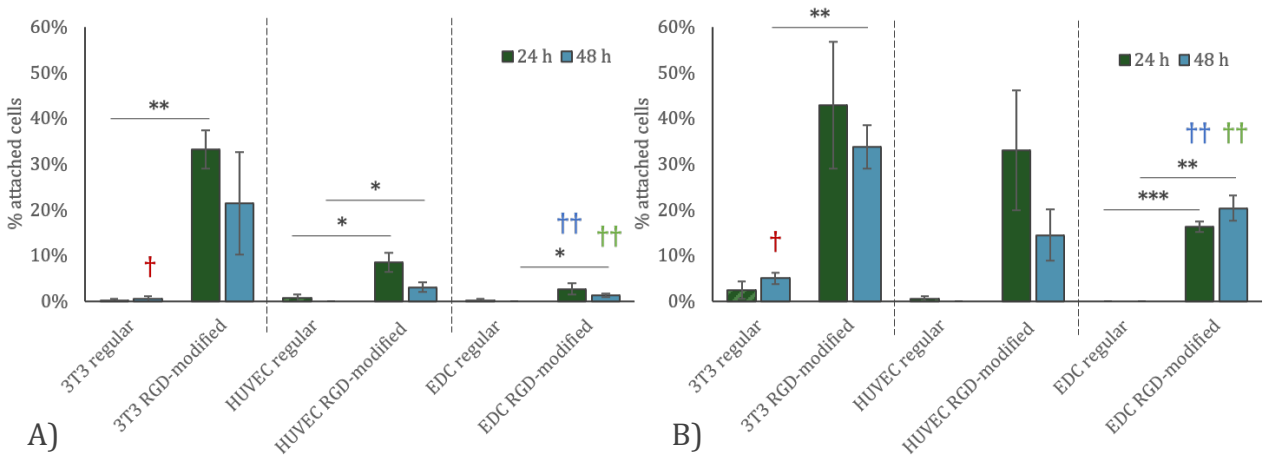

Figure 19 Plots of cell attachment to microcapsules. A) cell attachment to microcapsules incubated on regular culture dishes, B) cell attachment to microcapsules incubated in pHEMA coated dishes. Significant differences are seen between regular and modified agarose samples for most cell types. Association between pHEMA coating and increased cell attachment is also seen with EDC samples. Coloured daggers represent statical significance between samples between the two plots. $n \geq 3$ for all data points. Shown is mean ± SEM. * $p < 0.05$, ** $p < 0.01$, *** $p < 0.001$, † $p < 0.05$, †† $p < 0.01$.

3.6 Mixing Experiments

The results of mixing experiments between NIH 3T3 cells and empty agarose microcapsules are shown in Figure 20; image A shows mixing with RGD-modified agarose microcapsules, and image B shows mixing with regular agarose microcapsules. For experiments with RGD-modified agarose material, cells can be seen wrapping around and attaching to the microcapsules, whereas in the regular agarose samples, cells were much more aggregated, and showed no evidence of attachment or any association with the regular agarose microcapsules. The red arrows in Figure 20 A highlight the cells that were clearly associated and wrapped around the RGD-modified agarose microcapsules. For the cells that were attached to the microcapsules, they often attached in smaller aggregates, as shown in Figure 20 A on the right side, which made

it challenging to quantitatively determine the number of attached cells. Although these experiments did not provide quantitative data, they clearly showed that there is increased cellular adhesion with RGD-modified agarose compared to regular agarose and they provide further evidence that cells interact differently with a hydrogel that contains cell binding domains.

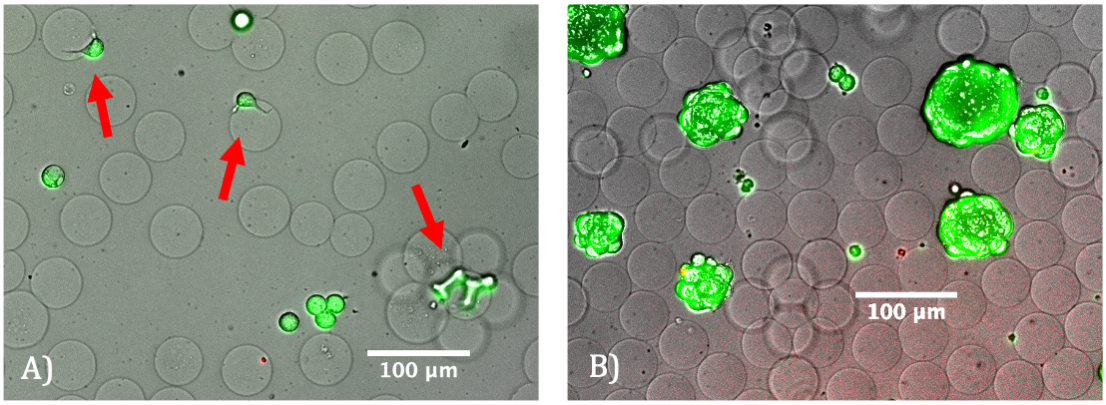

Figure 20 Cells mixed with empty agarose microcapsules. A) NIH 3T3s mixed with RGD-modified agarose microcapsules. Red arrows show cells that have attached to microcapsule surfaces. B) NIH 3T3s mixed with regular agarose microcapsules. Larger aggregates of cells formed and there was no indication any cell had associated or attached to the surface of microcapsules.

3.7 Confocal Imaging of Focal Adhesions

Confocal microscopy was performed on samples of cells encapsulated in RGD-modified agarose. The formation of cellular focal adhesions serves as an indicator of cell attachment to a surface. These focal adhesions are detected by observing accumulation of vinculin at the ends of actin filaments, and they would typically be observed along the cell membrane. EDCs were stained with multiple fluorescence dyes then viewed under a confocal microscope. In Figure 21 A, the FITC-conjugated secondary antibody to anti-vinculin is seen, showing the location of accumulations of vinculin along the cell membrane. Figure 21 B shows the DAPI stained nuclei of possibly two cells that have egressed and are seemingly attached to the microcapsules. The TRITC-conjugated Phalloidin is shown in Figure 21 C, mapping the location of the actin filaments within the cells. The orientation of these filaments is difficult to observe in this image, most likely

due to the 3D nature of the image, therefore the single focal plane not being able to capture the entire cell volume within this image. The brightfield image (Figure 21 D) clearly shows the cells lying outside a single microcapsule and contouring around the outside surface of multiple RGD-modified agarose microcapsules. The localized regions of vinculin around the outside of the cells, where they contact the surrounding microcapsules provides evidence that these structural focal adhesions are forming between the cells and the RGD-modified agarose, and a proper mechanical link is present in these samples.

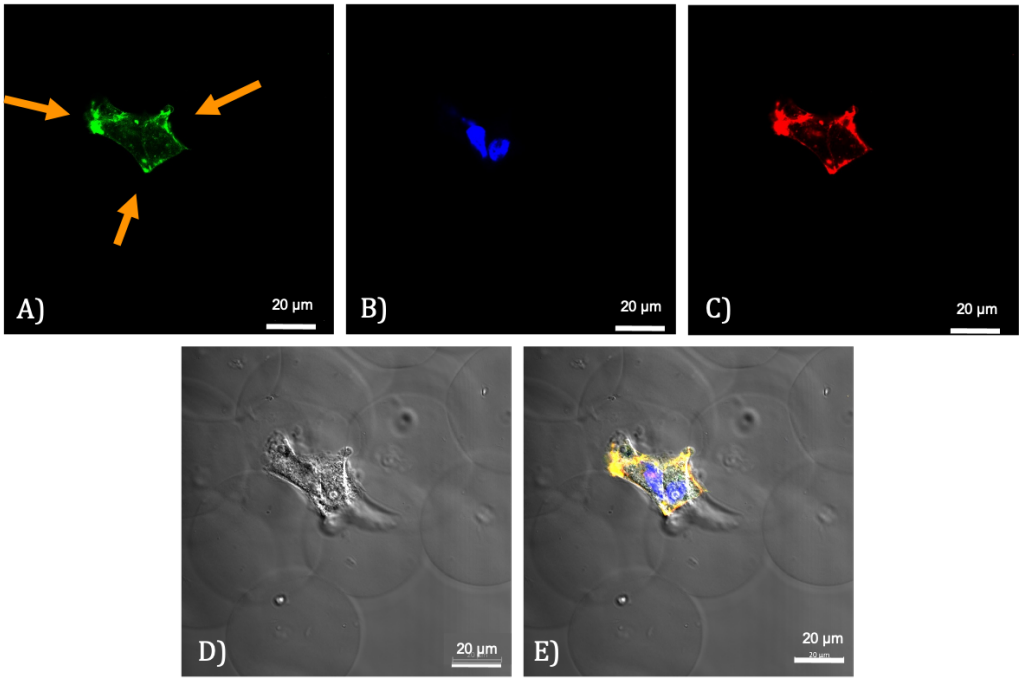

Figure 21 Images of an egressed EDC cell that was encapsulated in RGD-modified agarose and incubated for 24 h at 37˚C before fluorescent staining. A) FITC-conjugated secondary antibody to anti-vinculin, showing the location of vinculin, which is involved in the formation of focal adhesions. B) DAPI stained nuclei of two cells. C) TRITC-conjugated Phalloidin showing the location of actin filaments within the cell. D) Brightfield image of the egressed cells, clearly lying outside a microcapsule, and contouring around the surface of surrounding microcapsules. E) Overlaid image of each stain with the brightfield image.

4 CONCLUSIONS

Three major goals were achieved in this research project. First, I was able to determine that, by adding cell binding domains into agarose hydrogel used for cell microencapsulation, cells were able to attach to the outside of the microcapsules. These results are in stark contrast to cells encapsulated in regular agarose where essentially no attachment was observed. Second, I was able to quantitatively determine the number of cells that egressed the microcapsules and then attached to the outside of these microcapsules. Thirdly, I was able to show that this cell attachment behaviour is seen with multiple different cell types, including therapeutically relevant cell types.

A microfluidic device was used to encapsulate cells in regular agarose and in novel RGD-modified agarose. Fluorescence microscopy was used to analyze these samples at various timepoints up to 48 h after encapsulation to determine the cell viability, microcapsule occupancy, cell egress from microcapsules, and cell attachment to microcapsules. These tests were conducted in two different plate coating conditions; one with no coating, so that cells could adhere to the culture dish; and another with a pHEMA coating, for which cells could not attach to the culture dish, thereby mimicking an environment in which the surrounding tissue is not available for cell attachment. Since attachment is a key factor for cellular health, cell attachment is a key parameter for cell-based therapeutic strategies.

The results presented in this thesis show strong evidence that encapsulation of cells in RGD-modified hydrogels greatly increased cellular attachment to the outside of their microcapsule. Attachment of NIH 3T3 cells increased from 5% when encapsulated in regular

agarose to 35% when encapsulated in RGD-modified agarose, when studied in pHEMA coated plates. Similar trends were shown with the therapeutic cell lines in pHEMA coated plates, with HUVEC attachment increasing from 0% to 15% and EDC attachment increasing from 1% to 20% for regular agarose and RGD-modified agarose respectively. Investigating cellular attachment onto RGD-modified agarose microcapsules when incubated in regular cell culture treated plates versus pHEMA coated plates showed that attachment onto the hydrogel increased when the dish surface was not available for cell attachment. This data shows promise for *in vivo* studies which, in the past, have been limited by the lack of attachment of injected cells to surrounding tissues quickly and the swift clearing of the cells from this area.[3]

The novel RGD-modified agarose used in the studies provided here showed no negative effects on encapsulated cell viability. It is important that cells are encapsulated in a desirable environment, so that they are healthy and can provide the needed therapeutic effects.

Cell viability, as measured using the live/dead stain, was reduced from 76% to 72% for EDC cells encapsulated in RGD-modified agarose, 84% to 76% for HUVECs encapsulated in the same material, and NIH 3T3 cells increased cell viability from 75% to 81%, between the 2 h and 48 h timepoints, respectively.

The results presented here show great promise for use in cell-based therapeutic treatments. By increasing the number of cells associated with the microcapsules, it is hypothesized that cell retention will also increase as well. One of the main issues affecting current cell-based strategies is low retention and low engraftment of injected cells. Free floating cells injected into damaged tissues are very quickly cleared from this site, and therefore give limited therapeutic effects.[3] Encapsulation of therapeutic cells in hydrogels has been shown to increase

cellular retention at the injection site[3], but a high percentage of encapsulated cells still egress their encapsulation material.[6] After a cell has egressed its microcapsule within an unmodified hydrogel, it does not interact significantly with its microcapsule and is unlikely to remain at this site. The RGD-modified material used here, with added cell binding domains, helps to improve cell retention: cells attached to the outside of the microcapsules from which they egressed, providing a longer residence time that should result in improvements in the therapeutic effect.

5 FUTURE WORK

Further studies using this RGD-modified agarose material for cell encapsulation are needed. The data outlined here shows promise for use of this material *in vivo* but these studies still need to be conducted. Testing of therapeutic cells encapsulated in RGD-modified agarose in animal models are critical to understanding cellular behaviour in this much more complex environment. I have tested cell conditions that closely mimic an *in vivo* environment, but there are many more parameters that were not tested here, such as forces to which the cells are subjected to during injection and at the site of tissue damage, as well as a multitude of different surfaces and signals with which the cells will interact with. These animal tests are crucial for determining whether increased cell attachment does in fact increase therapeutic effects, such as scar tissue size, normal tissue functioning, angiogenesis, and many more.

Other optimization experiments also should be conducted to determine whether the number of egressed cells that attach to microcapsules can be increased. Previous studies suggest that increasing microcapsule diameter increases cell-mediated repair when used in damaged tissues, presumably due to increased cell-to-cell communication from within higher occupancy microcapsules.[3] Other studies have also suggested that hydrogel mechanical properties play a large role in cell viability within these materials.[76] Investigating material properties, especially mechanical properties such as gel strength at different concentrations of RGD-modified agarose and regular agarose may play an important role in creating an ideal environment for therapeutic cells.

Understanding the timeframe in which these cell types egress from the microcapsules and attach to the microcapsules is also important. For non-invasive treatments, these cells should be injected into the body and then travel to the damaged tissues, and therefore it is important to ensure that cells do not egress from the microcapsules before they arrive at the desired location. Controlling this time constant of the encapsulation material could have significant advantages for drug delivery systems and therefore is an interesting area to investigate further.

Eventually biodegradability of the hydrogel will be very important to focus on as well. Agarose does not degrade in the body and therefore will stay indefinitely if not modified with some biodegradable material. The present system uses a blend of two agarose types, low gelling agarose and RGD-modified agarose, and therefore is potentially easy to change this blend to include a known biodegradable material such as gelatin, or collagen. These new blends will need to be investigated to understand the timescale of degradation and cell behaviour within them, but a strategy to address the lack of current biodegradability of this agarose system will be necessary.

Cell adhesion is mediated by many different proteins, and signals, and other binding domains attached to the encapsulation material should also be investigated. Choosing the cell binding domain that is specific to a given cell type is advantageous to optimize each specific therapeutic treatment. We have considered a general method of increasing cellular retention that can be used for a wide range of cell types, and therefore a wide range of cell-based treatments, and this has many benefits. However, when focusing on a specific treatment, customized methods of cell binding should be designed.

REFERENCES

1. Davis, D. R. *et al.* Isolation and expansion of functionally-competent cardiac progenitor cells directly from heart biopsies. *J. Mol. Cell. Cardiol.* **49**, 312–321 (2010).
2. Smith, R. R. *et al.* Regenerative potential of cardiosphere-derived cells expanded from percutaneous endomyocardial biopsy specimens. *Circulation* **115**, 896–908 (2007).
3. Kanda, P. *et al.* Deterministic paracrine repair of injured myocardium using microfluidic-based cocooning of heart explant-derived cells. *Biomaterials* **247**, 120010 (2020).
4. Jones, M. K., Lu, B., Girman, S. & Wang, S. Cell-based therapeutic strategies for replacement and preservation in retinal degenerative diseases. *Prog. Retin. Eye Res.* **58**, 1–27 (2017).
5. Ma, J. *et al.* Concise review: cell-based strategies in bone tissue engineering and regenerative medicine. *Stem Cells Transl. Med.* **3**, 98–107 (2014).
6. Benavente-Babace, A., Haase, K., Stewart, D. J. & Godin, M. Strategies for controlling egress of therapeutic cells from hydrogel microcapsules. *J. Tissue Eng. Regen. Med.* **13**, 612–624 (2019).
7. Terrovitis, J. *et al.* Noninvasive Quantification and Optimization of Acute Cell Retention by In Vivo Positron Emission Tomography After Intramyocardial Cardiac-Derived Stem Cell Delivery. *J. Am. Coll. Cardiol.* **54**, 1619–1626 (2009).
8. Blocki, A. *et al.* Microcapsules engineered to support mesenchymal stem cell (MSC) survival and proliferation enable long-term retention of MSCs in infarcted myocardium. *Biomaterials* **53**, 12–24 (2015).
9. Mount, N. M., Ward, S. J., Kefalas, P. & Hyllner, J. Cell-based therapy technology

classifications and translational challenges. *Philos. Trans. R. Soc. B Biol. Sci.* **370**, (2015).

10. Heathman, T. R. *et al.* The translation of cell-based therapies: Clinical landscape and manufacturing challenges. *Regen. Med.* **10**, 49–64 (2015).
11. Buzhor, E. *et al.* Cell-based therapy approaches: the hope for incurable diseases. *Regen. Med.* **9**, 649–672 (2014).
12. Liang, X., Ding, Y., Zhang, Y., Tse, H. F. & Lian, Q. Paracrine mechanisms of mesenchymal stem cell-based therapy: Current status and perspectives. *Cell Transplant.* **23**, 1045–1059 (2014).
13. Hong, K. U. *et al.* C-Kit+ Cardiac Stem Cells Alleviate Post-Myocardial Infarction Left Ventricular Dysfunction Despite Poor Engraftment and Negligible Retention in the Recipient Heart. *PLoS One* **9**, 1–7 (2014).
14. *Functional biopolymers*. (Springer, 2019).
15. Kanda, P. *et al.* Deterministic Encapsulation of Human Cardiac Stem Cells in Variable Composition Nanoporous Gel Cocoons to Enhance Therapeutic Repair of Injured Myocardium. *ACS Nano* **12**, 4338–4350 (2018).
16. Mehregan Nikoo, A., Kadkhodaee, R., Ghorani, B., Razzaq, H. & Tucker, N. Controlling the morphology and material characteristics of electrospray generated calcium alginate microhydrogels. *J. Microencapsul.* **33**, 605–612 (2016).
17. Köster, S. *et al.* Drop-based microfluidic devices for encapsulation of single cells. *Lab Chip* **8**, 1110–1115 (2008).
18. Easley, C. J., Humphrey, J. A. C. & Landers, J. P. Thermal isolation of microchip reaction chambers for rapid non-contact DNA amplification. *J. Micromechanics Microengineering*

17, 1758–1766 (2007).

19. Sainiemi, L., Nissilä, T., Kostiainen, R., Ketola, R. A. & Franssila, S. A microfabricated silicon platform with 60 microfluidic chips for rapid mass spectrometric analysis. *Lab Chip* **11**, 3011–3014 (2011).

20. Ren, C. & Lee, A. *Droplet Microfluidics*. (The Royal Society of Chemistry, 2021). doi:10.1039/9781839162855

21. Cramer, C., Fischer, P. & Windhab, E. J. Drop formation in a co-flowing ambient fluid. *Chem. Eng. Sci.* **59**, 3045–3058 (2004).

22. Teh, S. Y., Lin, R., Hung, L. H. & Lee, A. P. Droplet microfluidics. *Lab Chip* **8**, 198–220 (2008).

23. Collins, D. J., Neild, A., deMello, A., Liu, A. Q. & Ai, Y. The Poisson distribution and beyond: Methods for microfluidic droplet production and single cell encapsulation. *Lab Chip* **15**, 3439–3459 (2015).

24. Lagus, T. P. & Edd, J. F. A review of the theory, methods and recent applications of high-throughput single-cell droplet microfluidics. *J. Phys. D. Appl. Phys.* **46**, (2013).

25. Blaesild, P. & Granfeldt, J. *Statistics with Applications in Biology and Geology*. (Chapman and Hall/CRC, 2002). doi:https://doi-org.proxy.bib.uottawa.ca/10.1201/9781315273662

26. Cao, Y. *et al.* Comparative study of the use of poly(glycolic acid), calcium alginate and pluronics in the engineering of autologous porcine cartilage. *J. Biomater. Sci. Polym. Ed.* **9**, 475–487 (1998).

27. Sims, C. D. *et al.* Tissue engineered neocartilage using plasma derived polymer substrates and chondrocytes. *Plastic and Reconstructive Surgery* **101**, 1580–1585 (1998).

28. Perka, C., Spitzer, R. S., Lindenhayn, K., Sittinger, M. & Schultz, O. Matrix-mixed culture: New methodology for chondrocyte culture and preparation of cartilage transplants. *J. Biomed. Mater. Res.* **49**, 305–311 (2000).

29. Nicodemus, G. D. & Bryant, S. J. Cell encapsulation in biodegradable hydrogels for tissue engineering applications. *Tissue Eng. - Part B Rev.* **14**, 149–165 (2008).

30. Chapter 2 - Components of the Immune System. in *Primer to the Immune Response (Second Edition)* (eds. Mak, T. W., Saunders, M. E. & Jett, B. D.) 21–54 (Academic Cell, 2014). doi:https://doi.org/10.1016/B978-0-12-385245-8.00002-9

31. Rowley, J. A., Madlambayan, G. & Mooney, D. J. Alginate hydrogels as synthetic extracellular matrix materials. *Biomaterials* **20**, 45–53 (1999).

32. Zarrintaj, P. *et al.* Agarose-based biomaterials for tissue engineering. *Carbohydr. Polym.* **187**, 66–84 (2018).

33. Imani, R., Emami, S. H., Moshtagh, P. R., Baheiraei, N. & Sharifi, A. M. Preparation and characterization of agarose-gelatin blend hydrogels as a cell encapsulation matrix: An in-vitro study. *J. Macromol. Sci. Part B Phys.* **51**, 1606–1616 (2012).

34. Dang, Q. F. *et al.* Characterization of collagen from haddock skin and wound healing properties of its hydrolysates. *Biomed. Mater.* **10**, 15022 (2015).

35. Jacques, E. *et al.* Collagen-Based Microcapsules As Therapeutic Materials for Stem Cell Therapies in Infarcted Myocardium. *ACS Biomater. Sci. Eng.* **6**, 4614–4622 (2020).

36. Lee, C. H., Singla, A. & Lee, Y. Biomedical applications of collagen. *Int. J. Pharm.* **221**, 1–22 (2001).

37. Mũnoz, Z., Shih, H. & Lin, C. C. Gelatin hydrogels formed by orthogonal thiol-norbornene

photochemistry for cell encapsulation. *Biomater. Sci.* **2**, 1063–1072 (2014).

38. Masters, K. S., Shah, D. N., Leinwand, L. A. & Anseth, K. S. Crosslinked hyaluronan scaffolds as a biologically active carrier for valvular interstitial cells. *Biomaterials* **26**, 2517–2525 (2005).

39. Chung, C., Mesa, J., Randolph, M. A., Yaremchuk, M. & Burdick, J. A. Influence of gel properties on neocartilage formation by auricular chondrocytes photoencapsulated in hyaluronic acid networks. *J. Biomed. Mater. Res. A* **77**, 518–525 (2006).

40. Hong, Y. *et al.* Covalently crosslinked chitosan hydrogel: Properties of in vitro degradation and chondrocyte encapsulation. *Acta Biomater.* **3**, 23–31 (2007).

41. Rice, M. A. & Anseth, K. S. Controlling cartilaginous matrix evolution in hydrogels with degradation triggered by exogenous addition of an enzyme. *Tissue Eng.* **13**, 683–691 (2007).

42. Gavenis, K., Schneider, U., Groll, J. & Schmidt-Rohlfing, B. BMP-7-loaded PGLA microspheres as a new delivery system for the cultivation of human chondrocytes in a collagen type I gel: The common nude mouse model. *Int. J. Artif. Organs* **33**, 45–53 (2010).

43. Martinsen, A., Skjåk-Bræk, G. & Smidsrød, O. Alginate as immobilization material: I. Correlation between chemical and physical properties of alginate gel beads. *Biotechnol. Bioeng.* **33**, 79–89 (1989).

44. Peppas, N. A. & Langer, R. S. *Biopolymers II*. (Springer, 1995).

45. Bella, J., Eaton, M., Brodsky, B. & Berman, H. M. Crystal and Molecular Structure of a Collagen-Like Peptide at 1.9 Å Resolution. *Sci. (American Assoc. Adv. Sci.* **266**, 75–81

(1994).

46. Deatherage, J. R. & Miller, E. J. Packaging and Delivery of Bone Induction Factors in a Collagenous Implant. *Coll. Relat. Res.* **7**, 225–231 (1987).

47. Dong, C. & Lv, Y. Application of collagen scaffold in tissue engineering: Recent advances and new perspectives. *Polymers (Basel).* **8**, 1–20 (2016).

48. Agarose. *Millipore Sigma* Available at: https://www.sigmaaldrich.com/CA/en/substance/agarose123459012366. (Accessed: 20th September 2021)

49. Lin, L. *et al.* Efficient cell capture in an agarose-PDMS hybrid chip for shaped 2D culture under temozolomide stimulation. *RSC Adv.* **6**, 75215–75222 (2016).

50. Meilander-Lin, N. J., Cheung, P. J., Wilson, D. L. & Bellamkonda, R. V. Sustained in Vivo Gene Delivery from Agarose Hydrogel Prolongs Nonviral Gene Expression in Skin. *Tissue Eng.* **11**, 546–555 (2005).

51. Suzawa, Y. *et al.* Regenerative behavior of biomineral/agarose composite gels as bone grafting materials in rat cranial defects. *J. Biomed. Mater. Res. - Part A* **93**, 965–975 (2010).

52. Awadhiya, A., Tyeb, S., Rathore, K. & Verma, V. Agarose bioplastic-based drug delivery system for surgical and wound dressings. *Eng. Life Sci.* **17**, 204–214 (2017).

53. Sakai, S. *et al.* Subsieve-size agarose capsules enclosing ifosfamide-activating cells: a strategy toward chemotherapeutic targeting to tumors. *Mol. Cancer Ther.* **4**, 1786–1790 (2005).

54. Jiang, C., Liu, Z., Cheng, D. & Mao, X. Agarose degradation for utilization: Enzymes,

pathways, metabolic engineering methods and products. *Biotechnol. Adv.* **45**, 107641 (2020).

55. Ingber, D. E. & Folkman, J. Mechanochemical switching between growth and differentiation during fibroblast growth factor-stimulated angiogenesis in vitro: Role of extracellular matrix. *J. Cell Biol.* **109**, 317–330 (1989).

56. Chen, C. S., Mrksich, M., Huang, S., Whitesides, G. M. & Ingber, D. E. Geometric control of cell life and death. *Science (80-.).* **276**, 1425–1428 (1997).

57. Bellis, S. L. Advantages of RGD peptides for directing cell association with biomaterials. *Biomaterials* **32**, 4205–4210 (2011).

58. Karp, G. *et al. Cell and Molecular Biology Concepts and Experiments*. (2013).

59. An, C. *et al.* Continuous microfluidic encapsulation of single mesenchymal stem cells using alginate microgels as injectable fillers for bone regeneration. *Acta Biomater.* **111**, 181–196 (2020).

60. Yu, J. *et al.* The use of human mesenchymal stem cells encapsulated in RGD modified alginate microspheres in the repair of myocardial infarction in the rat. *Biomaterials* **31**, 7012–7020 (2010).

61. Arya, N., Forget, A., Sarem, M. & Shastri, V. P. RGDSP functionalized carboxylated agarose as extrudable carriers for chondrocyte delivery. *Mater. Sci. Eng. C* **99**, 103–111 (2019).

62. Donetella, R. J. *et al. Biological Concepts of Health*. (Pearson Education, Inc. Custon, 2011).

63. Kumar, V., Abbas, A. K. & Aster, J. C. *Robbins Basic Pathology*. (Elsevier, 2013).

64. Yang, L. *et al.* ICAM-1 regulates neutrophil adhesion and transcellular migration of TNF-α-activated vascular endothelium under flow. *Blood* **106**, 584–592 (2005).

65. Mamdouh, Z., Chen, X., Plerini, L. M., Maxfield, F. R. & Muller, W. A. Targeted recycling of PECAM from endothelial surface-connected compartments during diapedesis. *Nature* **421**, 748–753 (2003).

66. Tilokee, E. L. *et al.* Paracrine Engineering of Human Explant-Derived Cardiac Stem Cells to Over-Express Stromal-Cell Derived Factor 1α Enhances Myocardial Repair. *Stem Cells* **34**, 1826–1835 (2016).

67. Virani, S. S. *et al.* Heart Disease and Stroke Statistics—2020 Update: A Report From the American Heart Association. *Circ. (New York, N.Y.)* **141**, e139–e151 (2020).

68. Fryar, C. D., Chen, T.-C. & Li, X. Prevalence of uncontrolled risk factors for cardiovascular disease: United States, 1999-2010. *NCHS Data Brief* 1–8 (2012).

69. Smith, R. R., Marbán, E. & Marbán, L. Enhancing retention and efficacy of cardiosphere-derived cells administered after myocardial infarction using a hyaluronan-gelatin hydrogel. *Biomatter* **3**, 29–34 (2013).

70. Luan, N. M., Teramura, Y. & Iwata, H. Immobilization of the soluble domain of human complement receptor 1 on agarose-encapsulated islets for the prevention of complement activation. *Biomaterials* **31**, 8847–8853 (2010).

71. Benavente-Babace, A. *et al.* Single-cell trapping and selective treatment via co-flow within a microfluidic platform. *Biosens. Bioelectron.* **61**, 298–305 (2014).

72. Tahvildari, R. *et al.* Manipulating Electrical and Fluidic Access in Integrated Nanopore-Microfluidic Arrays Using Microvalves. *Small* **13**, 1–7 (2017).

73. NIH/3T3 CRL-1658. *ATCC* (2021). Available at: https://www.atcc.org/products/crl-1658#:~:text=The NIH%2F3T3%2C a continuous,(ATCC CCL-163). (Accessed: 14th September 2021)

74. LIVE/DEAD Viability/Cytotoxicity kit, for mammalian cells. *ThermoFisher Scientific* Available at: https://www.thermofisher.com/order/catalog/product/L3224#/L3224. (Accessed: 26th September 2021)

75. Cell Counting Kit 8 (WST-8/CCK8). *Abcam*

76. Uludag, H., De Vos, P. & Tresco, P. A. Technology of mammalian cell encapsulation. *Adv. Drug Deliv. Rev.* **42**, 29–64 (2000).

6 SUPPLEMENTARY INFORMATION

6.1 Fluorescence Images Collected for Image Analysis

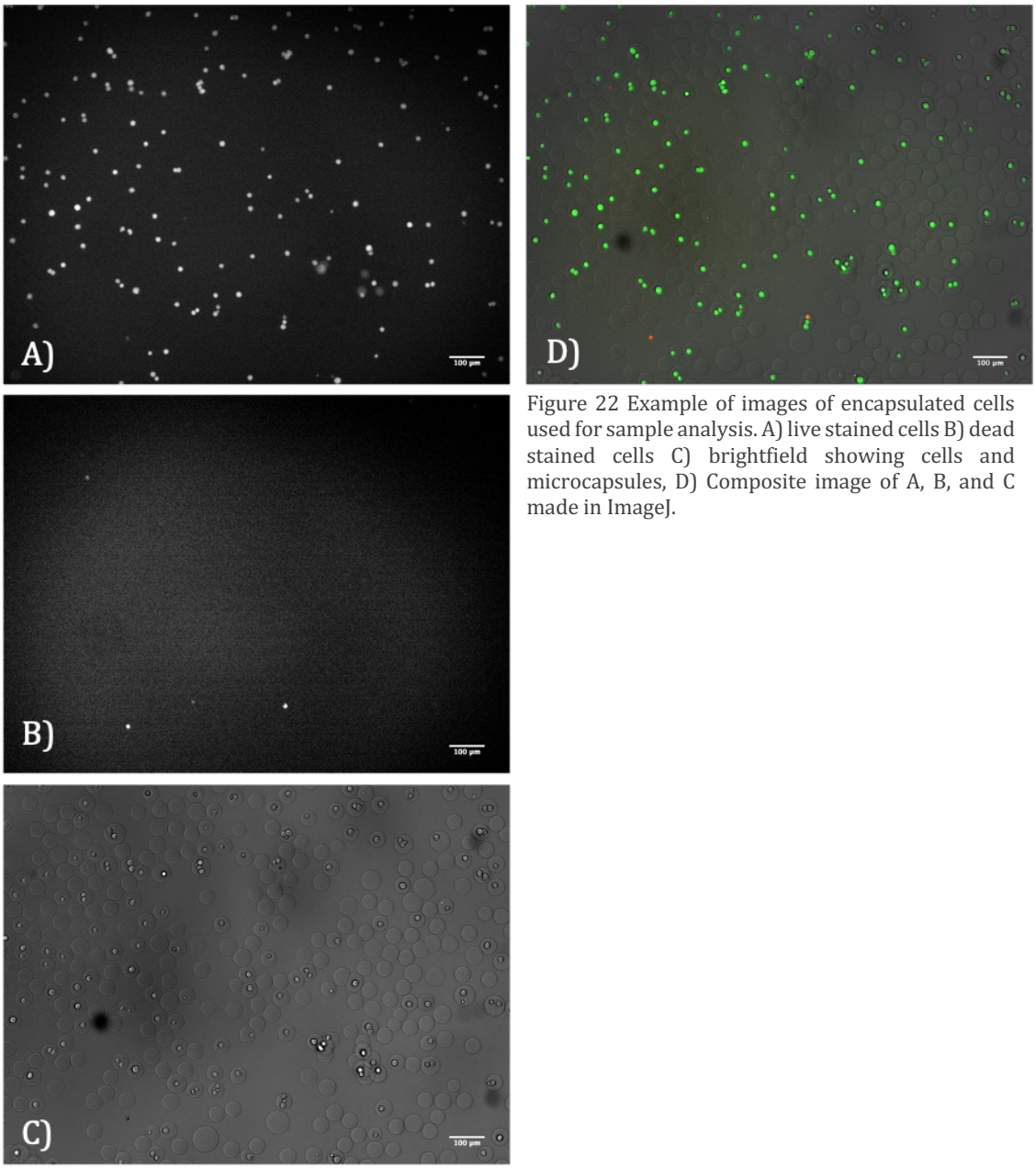

Figure 22 Example of images of encapsulated cells used for sample analysis. A) live stained cells B) dead stained cells C) brightfield showing cells and microcapsules, D) Composite image of A, B, and C made in ImageJ.

All images used for sample analysis were processed using the same protocol. Three images were collected for every composite image that was needed for proper image analysis. Without moving the microscope view, one image was collected using the FITC filter, one image was collected using the TRITC filter, and one image was collected using brightfield. The brightness and contrast were adjusted in ImageJ to optimize he visibility of the features within the images, and the "Merge

Channels" function in ImageJ was used to create a composite image with separate colours for each channel.

6.2 Heated Acrylic Box

This box was used to maintain an elevated temperature of the air surrounding the encapsulation setup to prevent the agarose from pregelling in the tubes that were attached to the microfluidic device. The box is made of acrylic plastic and the inside is covered in reflective foil thermal insulation. A heat strip was used to provide heating within the box, and it was attached to a heat sink with a small fan connected on the other side of the heat sink to circulate the heat radiating from the heat sink into the rest of the box. The heat strip was connected to an Omega Temperature Controller (CN63200-R1-LV). An external thermistor was also connected to this controller to provide feedback. The system temperature was set to 36 ˚C and measurements throughout the box showed this temperature was constant to within 1 ˚C.

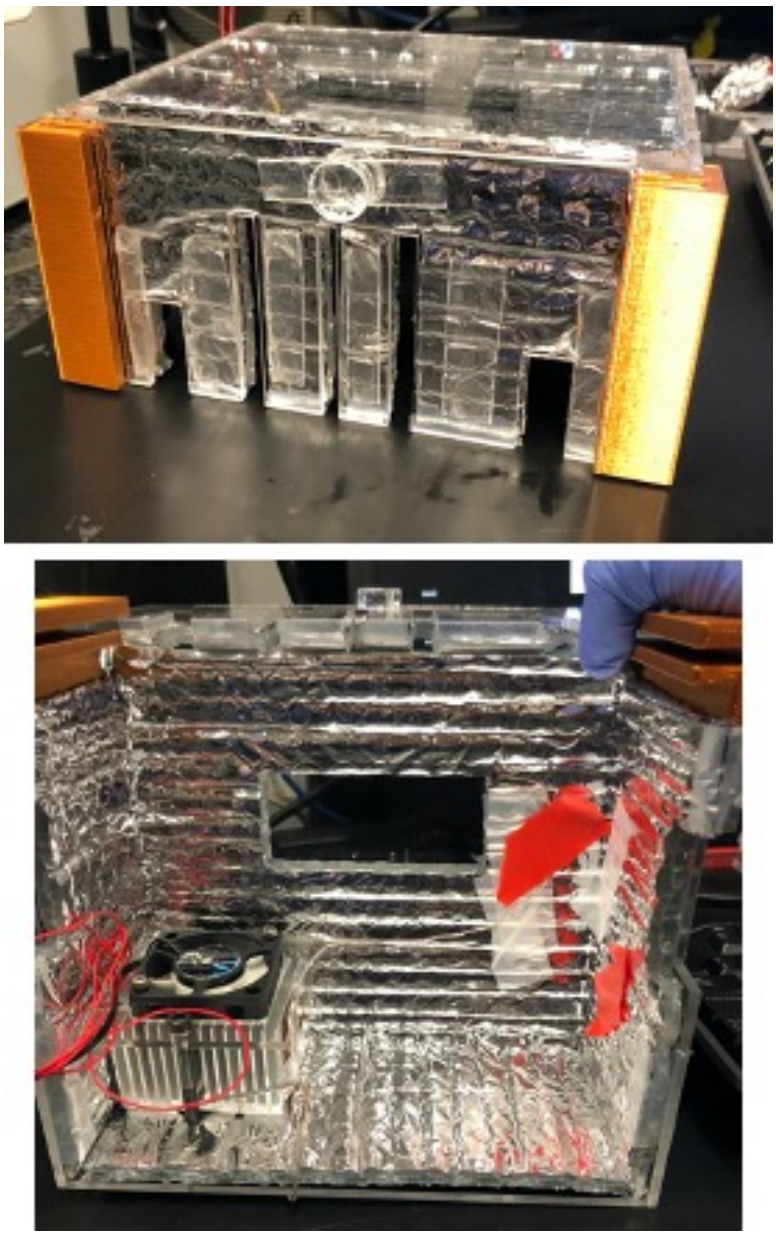

Figure 23 Images of heated acrylic box used to cover experimental setup to warm sample vials and tubing that enters the microfluidic device